HYBRID COMPUTER SIMULATION OF A MODEL FOR ELECTRIC LOAD SHORT-TERM FORECASTING

by

NICHOLAS C. STAVROULAKIS

MAJOR TECHNICAL REPORT

in

The Faculty

of

ENGINEERING

Presented in Partial Fulfillment of the Requirements for
the Degree of Master of Engineering at
Sir George Williams University
Montreal, Canada

AUGUST, 1974

HYBRID COMPUTER SIMULATION OF A MODEL FOR ELECTRIC LOAD SHORT-TERM FORECASTING

by

NICHOLAS C. STAVROULAKIS

ABSTRACT

This study presents a hybrid computer simulation of an electric load model for short-term forecasting. Chapter 1 summarizes the accomplished work in the form of an introduction. The necessary material for introducing the reader to the subject is included in Chapter 2. In the four sections of this chapter, load forecasting, a historical review, load behaviour and parameters affecting short-term load behaviour are discussed. Chapter 3 presents the discrete load model used and its system identification. The structure of the model is considered in section 3.1 where the two components (periodic, residual) constituting the load are presented. Section 3.2 summarizes the identification algorithm used, the resulting parameters and the performance of the discrete model. Chapter 4 contains the results of the hybrid simulation of the model. In Section 4.1, the transformation of the discrete model to an analog model is presented. The hybrid model implementation is discussed in Section 4.2, where the analog, digital and time control are considered separately. In Section 4.3, the model performance is described and its accuracy is discussed. The results show that the periodic part of the load needs to be described by more than the first 6 harmonics of the Fourier series, while the residual part can be made more accurate by using a higher order system. Finally, Chapter 5 presents the conclusions of this study, by summarizing the advantages and disadvantages of the model, its performance, as well as some suggestions for improvements and future work.

ACKNOWLEDGEMENTS

The author wishes to express his gratitude to Dr. V. Panuska for suggesting this project and for supervising this study.

In addition, I am deeply indebted to Dr. M. Vidyasagar for his criticism, corrections, advice, and valuable suggestions during the preparation of the thesis.

I also wish to express my thanks to Mr. P. Koutchouk for providing the data for this project as well as for discussions on some aspects of this study.

TABLE OF CONTENTS

LIST OF FIGURES

CHAPTER 1
INTRODUCTION

The objective of this study is the simulation of a model to be used for short-term forecasting of electrical power load. The starting point of this study is a model proposed by Galiana[1] and whose parameters were identified by Koutchouk.[2] This model consists of a difference equation, whose solution is added to a periodic function. The scope of this study is (i) transformation of the model into a form suitable for simulation on the hybrid computer, (ii) the actual simulation of the model, and (iii) comparison of the model's performance with actual data.

Chapter 2 provides the reader with background material in the field of load forecasting which is necessary for understanding this work. Section 2.1 summarizes the various categories of load forecasting and their applications, and the accuracy needed in a forecast. Section 2.2 presents a historical survey on load forecasting. In section 2.3, the load behaviour is discussed, and typical records of daily, weekly, seasonal, and annual load curves are presented. Finally, in section 2.4, the various parameters affecting short-term load behaviour are discussed.

Chapter 3 presents the load model structure, and its system identification. In section 3.1, the use of periodic and residual components in the model is justified. The periodic component accounts for

the aggregate customer requirements, and the residual component combines the effects of temperature together with an uncertainty term and a term reflecting the system dynamics. The system identification is discussed in section 3.2. The computational method used is outlined and the resulting system parameters are tabulated. In addition, performance of the discrete model is presented in the form of computer output plots.

Chapter 4 deals with the hybrid simulation of the load model. It begins by justifying the use of hybrid computing facility from the point of view of accuracy and repeatability provided by the digital computer, as well as the speed and realistic performance provided by the analog computer. Section 4.1 presents the transformation of the discrete model to an analog model. In section 4.2, the hybrid model implementation is described, considering separately the analog, digital and the interface units of the hybrid system. Amplitude and time scaling, as well as memory storage requirements, are considered. Section 4.3 presents the results obtained from the simulation in the form of analog computer plots. These graphs include input variables (temperature, noise), intermediate components (periodic, residual), and the output (simulated load). In addition, the difference between simulated load and actual load data is plotted to provide an idea of the accuracy of the model. The results are discussed and possible sources of errors are identified.

Finally, Chapter 5 concludes this study by presenting an evaluation of the model performance, possible improvements and suggestions for future work.

CHAPTER 2
BACKGROUND

2.1 Load Forecasting

In order to achieve a satisfactory management of a power utility, the generated output of the power plant must closely follow the power demand. However, power demand varies widely with time as well as spatially. Since generating units must be activated several hours before they can produce any power, it is important to have accurate forecasts of future load demands, in order for the power capacity to closely follow the demand.

There are many applications of load forecasting in the power industry. The main application is to load dispatching. By knowing the future load requirements in various areas, the power capacities of the various generating units can be adjusted to result in minimum operating cost. Also detection of dangerous operating conditions, and analysis of system contigencies, are easily handled when load flows in the immediate future can be accurately forecast. Preparation of maintenance schedules, selection of peacking capacity, geographic location of new power plants, and prediction of needs for main transmission links between generating plants and supply points, are all tasks which are easily handled with the help of accurate load forecasting.

Load forecasts may be classified into the following three categories:

(1) Short-term forecasts

(2) Medium-term forecasts

(3) Long-term forecasts

A forecast is considered to be short-term if its forecast period extends from a few minutes to a week, medium-term if the period is from a week to a season, and long-term when the period is longer than a season. Short-term forecasts are applicable in load dispatching operations and system security problems; medium-term forecasts are needed for maintenance schedules, while long-term forecasts find applications when new generating plants are required, or more generally when new investment in the power utility is under investigation.

Operational implementation of a forecasting procedure should satisfy two basic requirements. First, the computational methods should be simple and semi-automatic, because simplicity of computational methods reduces the computer storage and CPU time, while human interaction in the forecasting procedure usually provides higher accuracy in the forecast. Secondly, the accuracy of the forecast throughout the lead time period should meet prespecified requirements. The accuracy needed in a forecast varies according to the different forecasting categories. Thus, a short-term forecast requires greater accuracy than a medium-term forecast. In short-term forecasting the most important quantities are the daily maxima and minima. A daily peak error of between 1 and 3 percent on the total system load is considered to be satisfactory in short-term forecasting.

2.2 A Historical Survey

It is considered worthwhile to present some remarks regarding the historical development of the field of load forecasting. However, it should be emphasized that the following remarks are not intended to constitute a complete review of the extensive work in this area. Rather, the intention is to provide the reader with a historical perspective, which would give some feeling about the evolution of load forecasting.

Systematic load dispatching had its origins in the United States in the early 1930's. A few years later the methods developed in the United States were introduced, first in England and France, and then in other European countries. Since load dispatching operations require an accurate prediction of the future power demand, the problem of load forecasting soon became important.

One of the primary problems associated with load forecasting is the effect of weather on the power demand. In 1944, Henry Dryar,[3] a chief load dispatcher in Philadelphia Electric Company, published the first integrated article on the effects of weather on a system load. Since then, most of the people concerned with load forecasting attempted to emperically establish mathematical relationships between weather and power demand. This type of work was first introduced in the literature by M. Davies[4] in 1958. A similar attempt by G. Heinemann et. al.[5] followed in 1966, where they used regression analysis to derive a relationship between weather and power demand during summer months. Application of these relationships to load forecasting was found to introduce mathematical complications. To simplify the mathematics involved, some people

neglected the effects of weather completely while others considered only the effects of temperature on system load. This latter approach offered satisfactory results. Particularly in 1971, Galiana[6] used a method based partly on Dryar's work to account for only temperature variations. This method of Galiana is used in our study, and it is shown to be not only mathematically manageable, but also to simulate the temperature effects to an acceptable degree of accuracy.

A major breakthrough in the research on load forecasting came when probabilistic methods were used to takle the problems of uncertainty. Latham et. al.[7] pioneered this method in 1966. Subsequent researchers used techniques of state estimation, stochastic approximation, pattern recognition, Markov processes, separation algorithms and spectral analysis in order to develop forecasting procedures and models mainly for short-term forecasting. In 1968 Matthewman et. al.[8] considered the electricity demand as a time series, and they attempted to use only past load data through spectral expansion. In addition they used some pattern recognition techniques, which did not give very satisfactory results. At the same time Farmer and Potton[9] published another article in which the load was analysed through spectral expansion and Markov processes. In 1969 Inoue and Toyoda[10] were the first to use Kalman filtering techniques and separation algorithms for system and observation noise. Three interesting publications appeared in the literature in 1970. Schweppe and Wildes,[11] Toyoda et. al.[12] and Larson,[13] considered different problems in state estimation by using sequential filters, and constructed an algorithm to derive the parameters of system and observation noise, by using observed data series.

In 1971 Christiaanse[14] used exponential smoothing to develop an adaptive forecasting system, based on observed values of hourly demand. At the same time Galiana[16] wrote a Ph.D. thesis on load forecasting and system identification, in which he proposed a load model structure, which can be used for all types of forecasts. Subsequently, Koutchouk and Panuska[16] introduced a stochastic approximation algorithm of the recursive-least-squares type for the parameter identification of Galiana's model.

In 1973 two interesting papers dealing with long-term forecasts appeared in the literature, by Davey et. al.[17], and by Corpening et. al.[18] Both papers reflect the interest developing in load forecasting in the Electric Power Industries. Long-term forecasts seem to attract particular attention since they are expected to offer economic advantages in system planning.

2.3 Load Behaviour

A study of load behaviour is the first step towards load forecasting. Load behaviour is usually classified and studied in the following time periods:

1) hourly
2) daily
3) weekly
4) seasonal
5) annual

Consideration of items (1), (2), and (3) should be taken when one is dealing with short-term forecasts. Items (4) and (5) are usually

considered for medium forecasts, while anything longer comes into long-term forecasts. Hourly load behaviour is of no great importance in load forecasting, when forecasts are used to reserve and allocate spinning generation. During this time the only information provided about the load is the small random variations around an average trajectory. Since these variations cannot be followed by the spinning generation, they are only important in system security problems.

The daily load behaviour exhibits the most regular pattern of any load behaviour. Figure 2.1 shows a typical daily load curve. This load curve clearly represents the different levels of activity during the day.

The typical weekly load curve is shown in Figure 2.2. This pattern repeats itself in a regular manner provided all conditions are the same from week to week. Load curves from successive weeks tend to be similar, but this similarity is greatly reduced if the load time periods are more than three weeks apart. The load pattern over a weekly period shows a difference in load magnitudes between weekdays and the weekend. This fact is obviously due to large changes in the activity levels and patterns of the population during weekends.

A typical seasonal load curve is shown in Figure 2.3. The load level at any given time is partially uncorrelated from the past. Considering for example the load curve shown in Figure 2.3, one can distinguish two components, (1) the mean value of the load, and (2) some amount of uncertainty about the mean value which reflects the temperature changes.

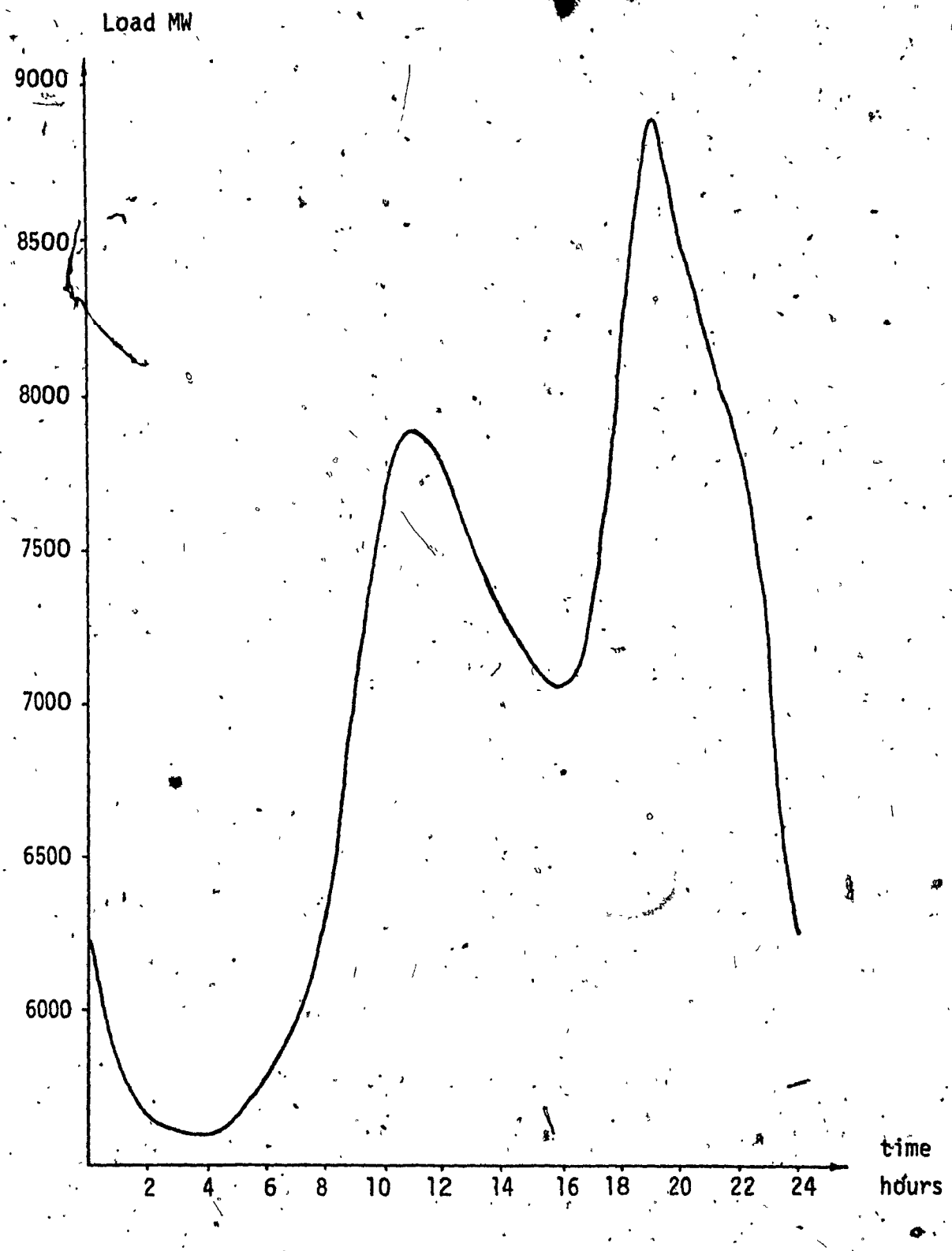

FIG. 2.1 - TYPICAL DAILY LOAD CURVE

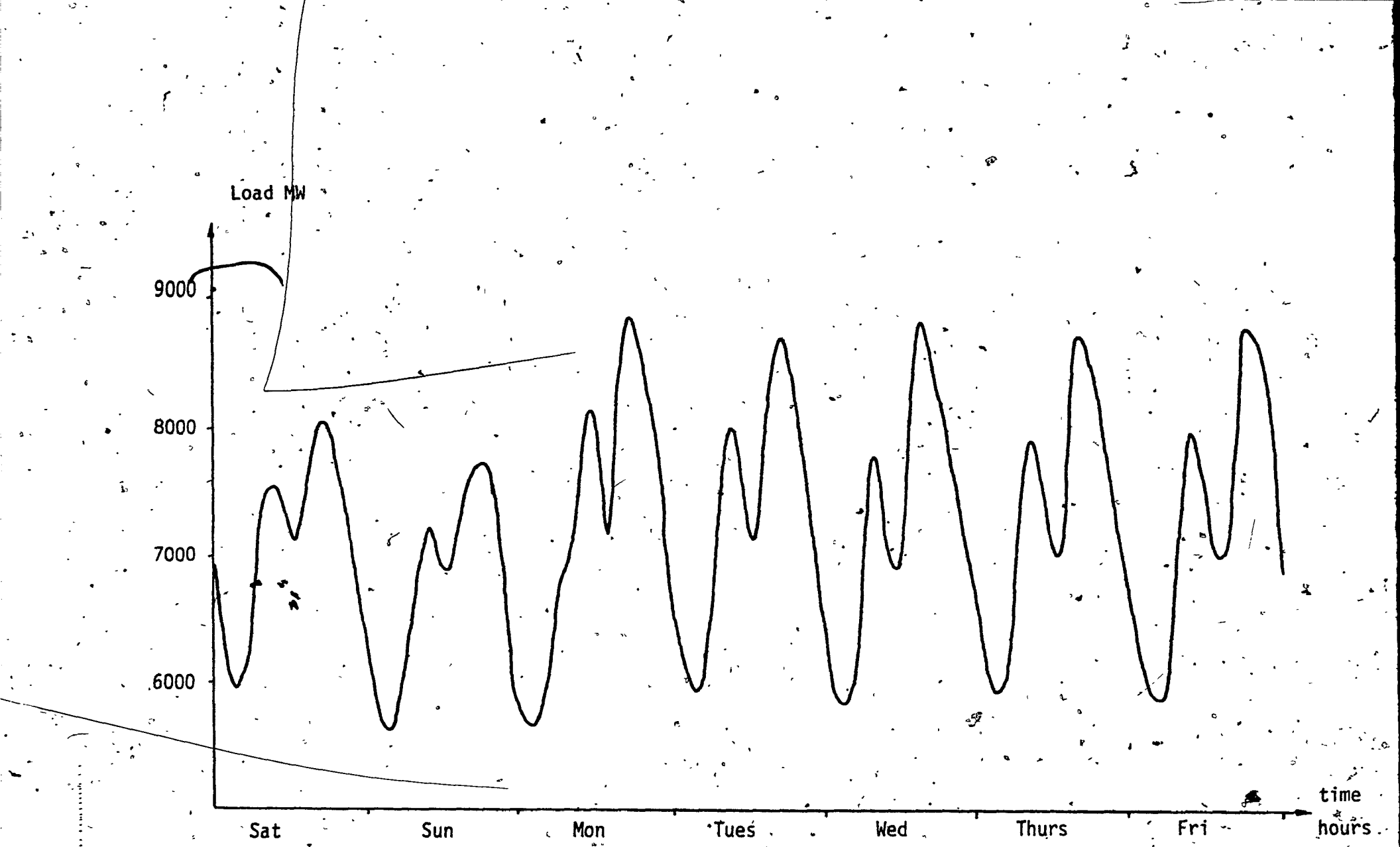

FIG. 2.2 - TYPICAL WEEKLY LOAD CURVE

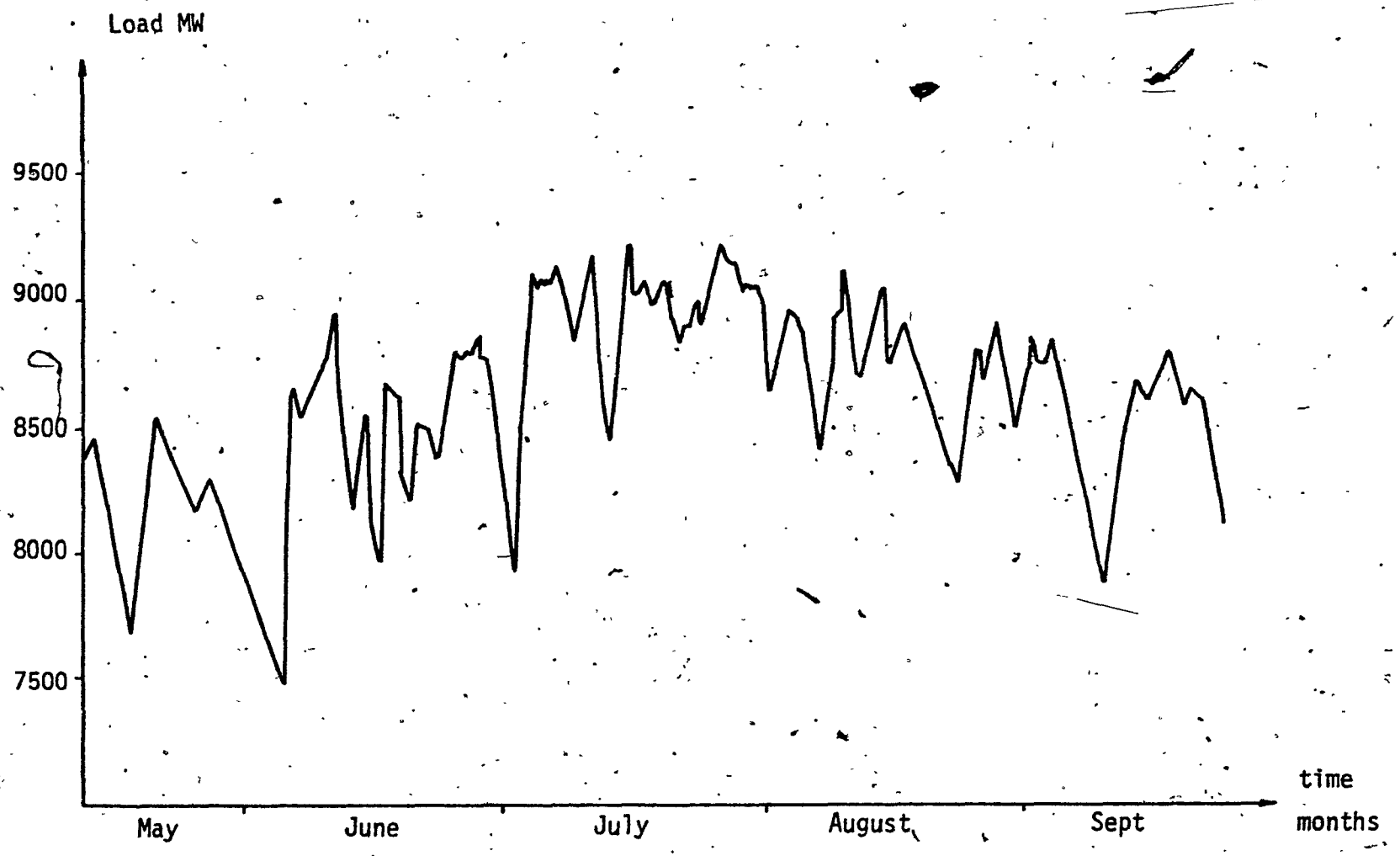

FIG. 2.3 - TYPICAL SEASONAL LOAD CURVE

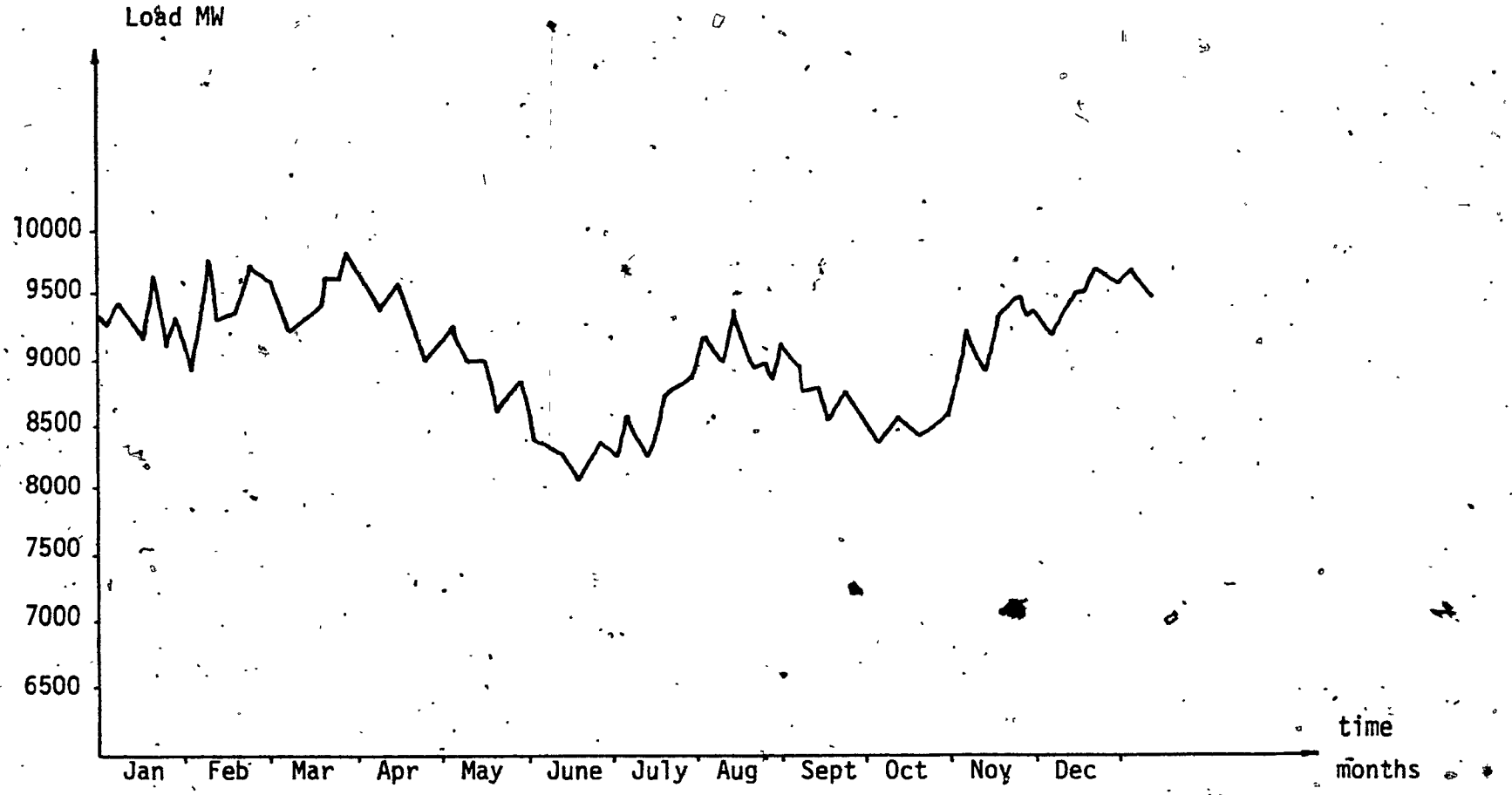

FIG. 2.4 - TYPICAL ANNUAL LOAD CURVE

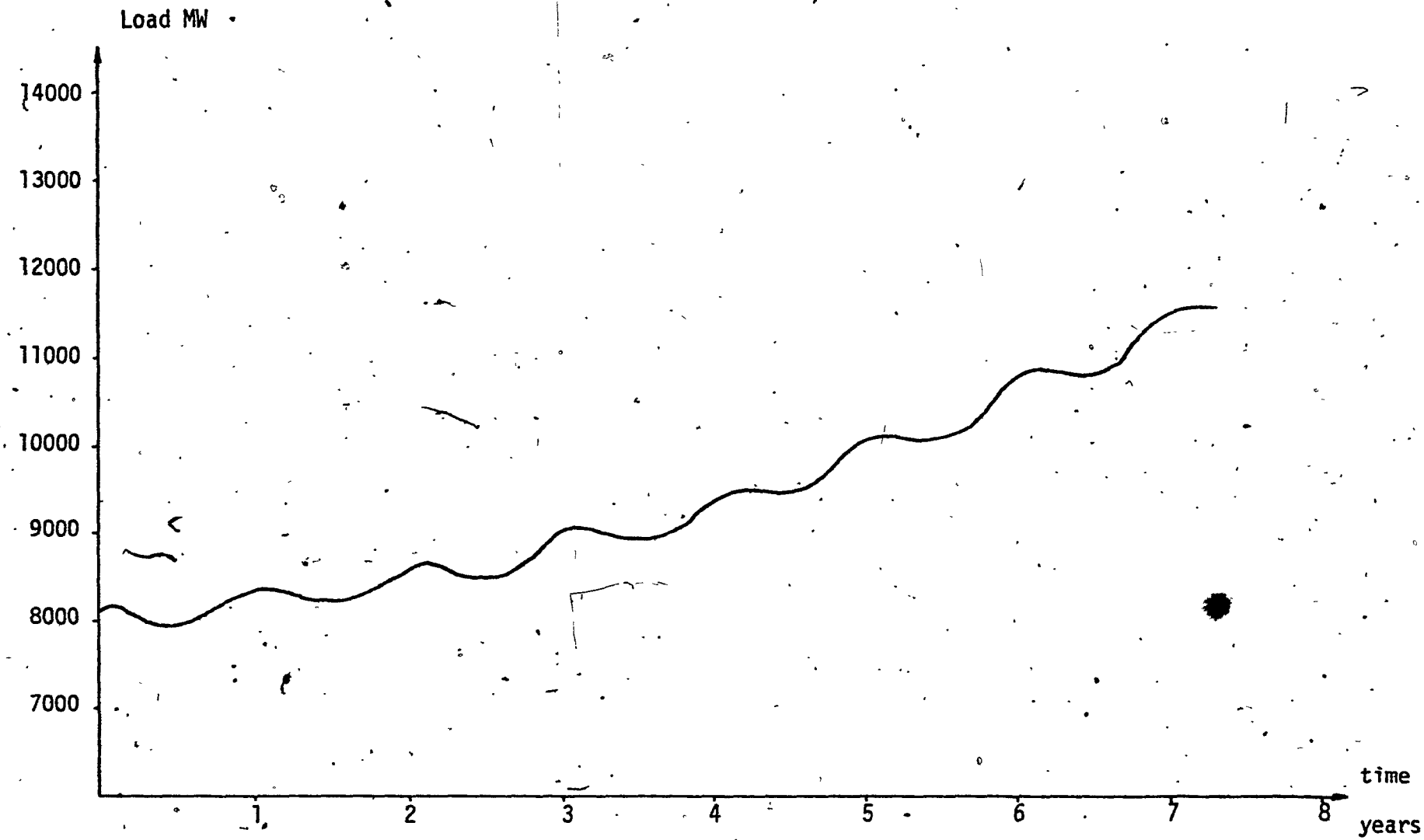

FIG. 2.5 - LOAD BEHAVIOUR OVER A FEW YEARS

Annual load behaviour is considered when forecasting is used to plan maintenance schedules or the construction of new generating units. The main characteristic of this pattern is a decrease in demand during the summer months and an increase during the winter months. A typical annual load record is shown in Figure 2.4. The load is largely determined by weather conditions, changes in consumer requirements, and specific events such as political, military, and social developments in the area.

The load curve over the span of a few years reflects the economic growth of the area under consideration. A typical relationship between time and demand is shown in Figure 2.5 The periodic part accounts for the annual load variations, which is superimposed over an exponentially increasing load, representing the increase in average power demand over the years.

2.4 Parameters Affecting Short-Term Load Behaviour

The load is a time varying process, the prediction of which always involves some uncertainty. The demand at any particular time is directly determined by the consumer actions which are influenced by various conditions, such as weather, social and economic status, industrial development, as well as living patterns associated with the use of electricity.

Short-term load behaviour is mostly influenced by the living patterns of the consumers and weather conditions. The effects of socio-economic status and industrial development do not come in to the picture, since their change during the period over which the load behaviour is considered, is almost unnoticeable. The living patterns of the consu-

mers associated with the use of electricity are called the aggregate customer requirements. These requirements are directly reflected in the load, in the form of hourly fluctuations. The daily load pattern is an example of these fluctuations over a period of one day. Weather conditions are reflected in the load behaviour, in the form of slow variations characterized by a time delay varying from 4 to 8 hours.

2.4.1 AGGREGATE CUSTOMER REQUIREMENTS

In order to study the effects of aggregate customer requirements on the system load, it is convenient to consider the public requirements separately from the industrial and commercial requirements.

(a) PUBLIC REQUIREMENTS: Daily load behaviour is an example of the effect of aggregate public requirements on the total power demand. This behaviour is basically periodic with a 24 hour period, and represents the consumer habits of work, sleep, rest, eating, etc. However, public consumer habits change according to the nature of the weekday. Thus, in the weekly load behaviour, a weekday's load demand differs greatly from the demand during weekends. A similar kind of difference in power demand occurs during holiday periods. In particular, during these non-working periods, sleeping hours are increased in the morning and reduced at night, breakfast, dinner and supper hours do not follow the regular pattern, while subway transportation is reduced. This accounts for a magnitude reduction in the load, as well as a shifting in time. Finally, it should be noted that radio and T.V. broadcasts of special interest increase the load considerably.

(b) INDUSTRIAL AND COMMERCIAL REQUIREMENTS: This category of consumer requirements is easily analyzed for short-term load behaviour. In fact, industry has an almost constant demand for every working day, while during holiday periods the demand either drops to zero or maintains a well-known behaviour. Thus, forecasting this component of the total load is a simple matter if weekly load records are available.

2.4.2 EFFECTS OF WEATHER

Weather fluctuations around normal weather conditions introduce variations in the power demand. These variations can range from a few MW to 1000 MW depending on the magnitude of the weather fluctuations. Among the different weather elements whose variations affect load behaviour, the major ones are:

1) Temperature
2) Light intensity
3) Humidity
4) Wind speed
5) Precipitation

The effect of temperature on the load is the most significant since it is mainly the temperature that controls the heating and cooling demands in a residential area. Light intensity is rated second in significance, and determines the extent of artificial lighting, which is a component of the total power demand. Humidity, wind speed and precipitation affect load indirectly, by changing the effective temperature. For example, atmospheric humidity above normal increases cooling demand, while wind speed and precipitation increase heating demand. Since the effect of temperature on load behaviour is much larger than the other

effects, in this study we consider only the effects of temperature in modelling the weather effects on system load. Furthermore, neglecting the effects of the other weather elements simplifies the mathematical formulations and the model structure. To account for temperature effects on load behaviour, a basic demand is defined at 65^0 F. As temperature increases, the demand for electric power increases indicating the use of cooling devices, and a similar increase in demand is noticed as the temperature decreases, indicating the use of heating devices. An extensive work on the effect of weather on system load is presented by Dryar[19] and Davies.[20]

CHAPTER 3
LOAD MODEL & SYSTEM IDENTIFICATION

3.1 Load Model Structure

The structure of the load model employed in this study is the one first developed by Galiana[21] with some minor modifications introduced by Koutchouk and Panuska.[22] In order to provide the reader with a clear picture of the model, a description of its structure is presented.

The load model is intended to be used for short-term load forecasting. In particular it is desired that the predictions of the model differ by no more than 3% from the actual load behavior, during regular weekdays. The inputs to the model are the temperature variations over the residential area, and a noisy signal representing the uncertainty in the system. Figure 3.1 shows a schematic diagram of the model. The model consists of two subsystems A and B. The function of subsystem A is to generate a periodic function $Y_p(t)$, which represents the deterministic component of the total load. The inputs to subsystem B are a noise input representing the uncertainties in the system, and a temperature dependent function, while its output is the residual load component $Y_r(t)$, which represents the fluctuations of the load about the periodic component $Y_p(t)$.

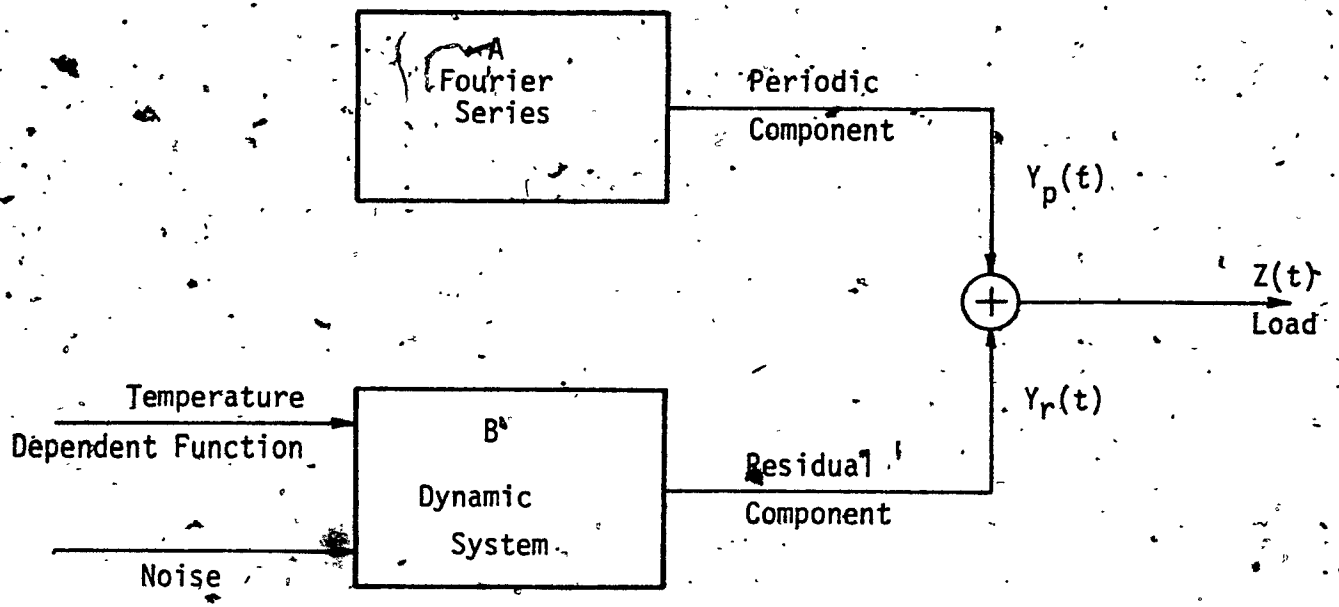

FIG. 3.1 - BLOCK DIAGRAM OF THE LOAD MODEL

The output of the model, representing the simulated load is given by

$$Z(t) = Y_p(t) + Y_r(t) \tag{3.1}$$

3.1.1 Periodic Component

In the typical weekly load curve, the load rises and falls at approximately the same time each day. Thus, the daily load curve repeats itself in a regular manner, which justifies the inclusion of a periodic component, with a period of 24 hours, as a component of the total load. The periodic component $Y_p(t)$ can be expressed as Fourier series in time with a period T_p = 24 hours, as follows:

$$Y_p(t) = d_0 + \sum_{i=1}^{n_p} \left[d_i \sin \left(\frac{2\pi i}{T_p}\right) t + d_{n_p+i} \cos \left(\frac{2\pi i}{T_p}\right) t \right] \tag{3.2}$$

Defining $$\omega = \frac{2\pi}{T_p} = 0.2617 \text{ rad/hour} \tag{3.3}$$

equation (3.2) can be written as,

$$Y_p(t) = d_0 + \sum_{i=1}^{n_p} \left[d_i \sin \omega i t + d_{n_p+i} \cos \omega i t \right] \tag{3.4}$$

The number and the values of the Fourier coefficients are determined using system identification procedures.

3.1.2 Residual Component

This component is included in the load to account for the uncertainty of the process, and the temperature effects. Since a power plant never experiences "normal" conditions, it is important to include

this component in the total simulated load, in order for the model to accurately reflect observed load behaviour. On the other hand, temperature influences the load level over the period of forecasting. Therefore, including a temperature dependent function is the best way to simulate the slow load variations due to temperature changes.

A possible description of the residual component is given by

$$Y_r(t) = e(t) + f_1\left(U(t)\right) + f_2\left(Y_r(t)\right) \qquad (3.5)$$

where the functions f_1 and f_2 are linear, $e(t)$ is a term representing the uncertainty in the system, and $U(t)$ is a temperature dependent function. By studying in detail the physics of the process, the nature of the various functions appearing in equation (3.5) can be determined.

(i) TEMPERATURE

To account for the effect of temperature on the simulated load, the method of weights as first suggested by Dryar[23] can be used. However, in this study, we follow a more realistic and simpler approach developed by Galiana,[24] and shown by him to provide a good approximation to the temperature effect on the system load.

According to Galiana, in order to generate the temperature dependent function $U(t)$, a normal daily temperature curve , $\bar{T}$, is first defined. This curve is obtained by averaging daily temperatures at hourly intervals for every month, and over a period of 10 years or more. A typical shape of this curve is shown in Figure 3.9. It is approximately periodic with a period of 24 hours. The periodicity of this curve makes this method powerful, since its shape contains the fact that temperature drops during the night-time and it increases during the

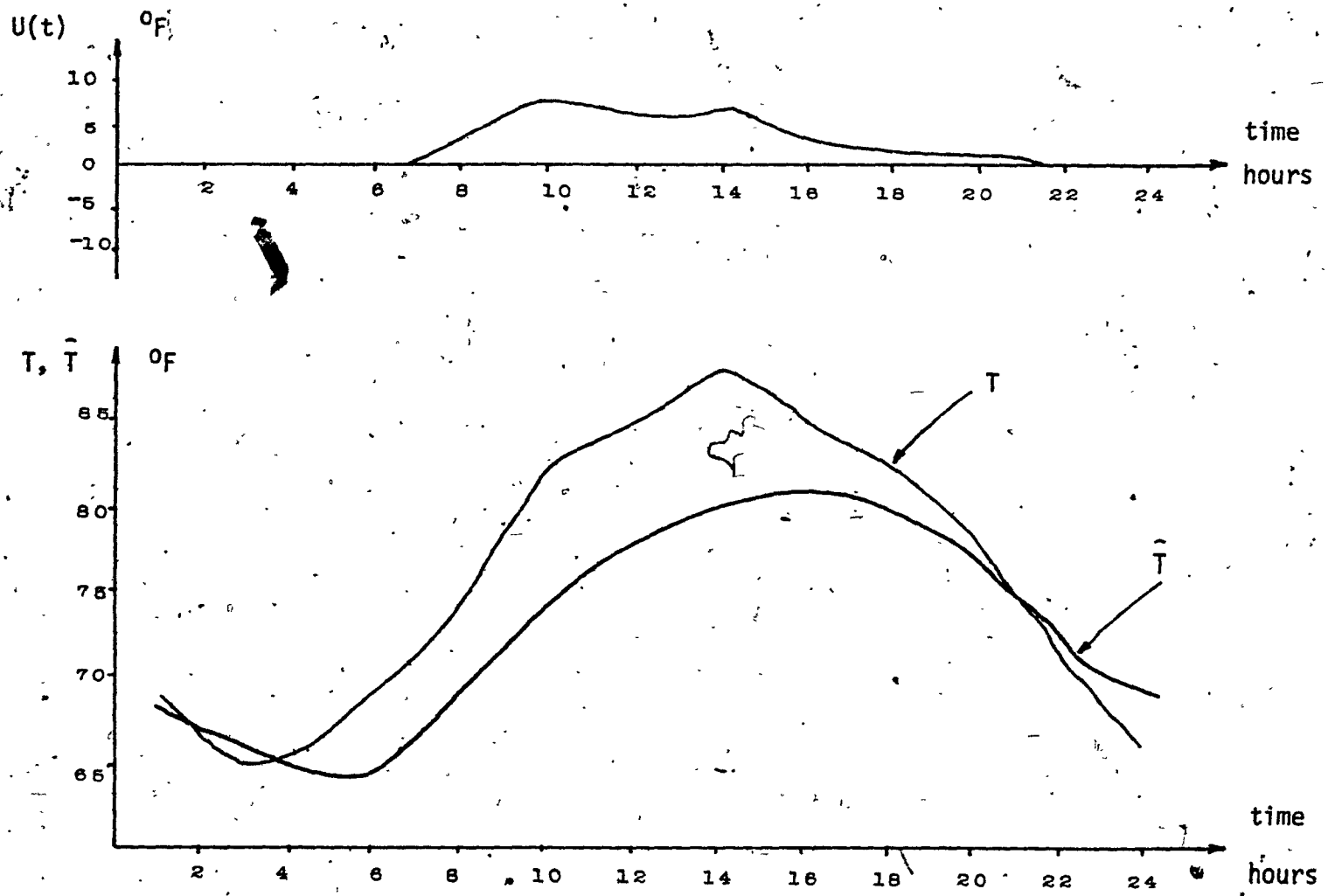

FIG. 3.2 - TYPICAL CURVES FOR NORMAL DAILY TEMPERATURE $\hat{T}$, ACTUAL DAILY TEMPERATURE T, AND TEMPERATURE DEPENDENT FUNCTION U(t)

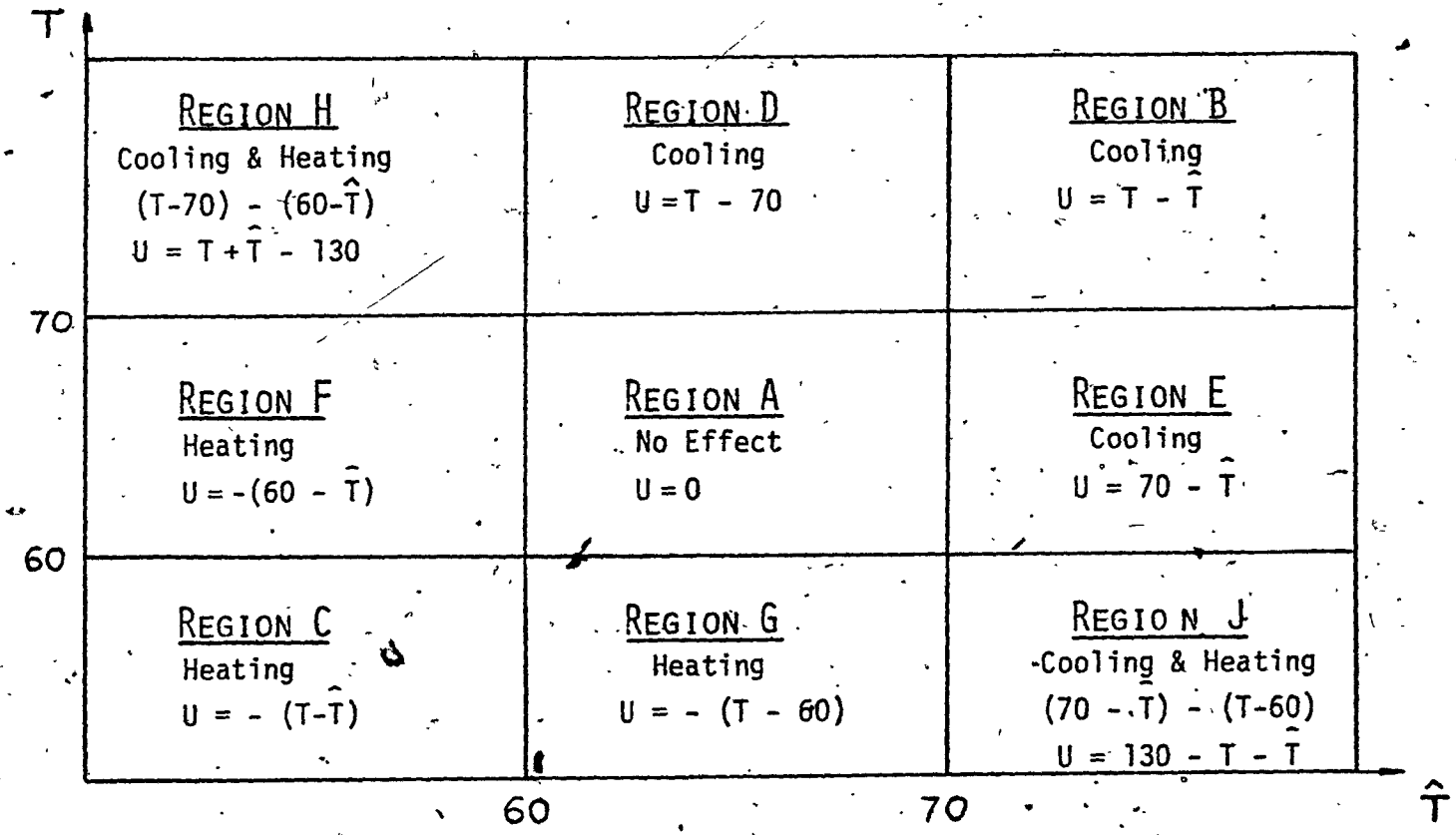

FIG. 3.3 - DEFINITION OF TEMPERATURE DEPENDENT FUNCTION U(t)

daytime. Therefore the periodic nature of the load, due to large changes in temperature between day and night, are included in the periodic component $Y_p(t)$. The temperature fluctuations about the normal daily temperature result in relatively small load variations, which justifies the use of a linear relationship between $Y_r(t)$ and $U(t)$.

The difference between actual hourly temperature, T, and normal daily temperature at that hour, $\hat{T}$, gives the value of the function $U(t)$. In Figure 3.3 the cartesian diagram as presented by Galiana[25] defines the temperature dependent function $U(t)$. This diagram is based on the fact that if the normal temperature, $\hat{T}$, is high, positive deviations in T from $\hat{T}$ will increase the load, indicating the use of heating devices. In order to separate these two regions, a zone between 60^0F and 70^0F is assumed to exist in which most people feel comfortable. As seen from Fig. 3.3, temperatures in region A have no effect on the load. Region B is a purely cooling region in which positive U's increase the load, while in the heating region C, negative U's increase the load. In regions D and G the normal temperature lies in the comfortable zone and only deviations of the actual temperature from this zone have effect on U. In regions E and F the actual temperature lies in the comfortable zone and therefore only deviations of the normal temperature are considered. In regions H and J the cooling and heating demand is mixed. These situations occur in fall and spring where the actual temperature lies far from the daily normal temperature.

The relation between $U(t)$ and $Y_r(t)$ is postulated on the basis of two assumptions: First that their relation is linear, and secondly that the effect of $U(t)$ on the load does not occur instantaneously but

is spread out over several hours. Therefore, the term $f_1(U(t))$ can be taken to be of the form

$$f_1(U(t)) = \sum_{j=1}^{m} b_j U(t-j) \quad (3.6)$$

where b_j ($j = 1, 2, \ldots m$) are constant coefficients. The number m and the values of b_j's are determined via the identification process.

(ii) UNCERTAINTY

There are many uncertainties in the load behaviour. The effects of weather elements other than temperature, uncertainties in the behaviour of the consumer, and imperfections in the model, to mention only a few, justify the inclusion of the term e(t) in the residual component.

The uncertainty term e(t) has zero mean and it is correlated with itself only up to some time difference, T_e. This can be expressed as

$$E\{e(t)\} = 0 \qquad \forall\, t \quad (3.7)$$

$$E\{e(t) \cdot e(\tau)\} = R_e(t-\tau) \quad (3.8)$$

where

$$R_e(t-\tau) = 0 \text{ wherever } |t-\tau| > T_e$$

For the sake of ease of identification, it is further assumed that e(t) consists of a linear combination of white noise terms, i.e.

$$e(t) = W(t) + \sum_{i=1}^{\ell} c_i\ W(t-i) \quad (3.9)$$

where

$$E\{W(t)\} = 0 \quad (3.10)$$

$$E\{W(t) \cdot W(\tau)\} = \delta(t-\tau) \quad (3.11)$$

(iii) SYSTEM DYNAMICS

The dynamics of the system dictate the form of the third term in equation (3.5). This term models the autocorrelation of the load.

Since the system load is causal, a simple way to account for the system dynamics is to define,

$$f_2(Y_r(t)) = \sum_{k=1}^{n} a_k \; Y_r\,(t - k) \qquad (3.12)$$

For the forecasting period, the coefficients a_k ($k = 1, 2, \ldots n$) are assumed to be constant, and their identification is discussed in the following section.

In summary, the residual component of the load can now be written analytically as,

$$Y_r(t) = W(t) + \sum_{i=1}^{\ell} c_i W(t - i) + \sum_{j=1}^{m} b_j U(t - j) + \sum_{k=1}^{n} a_k Y_r(t-k) \qquad (3.13)$$

3.2 SYSTEM IDENTIFICATION

In order to identify the Fourier coefficients in equation (3.4) and the parameters in equation (3.13), Koutchouk and Panuska[26] used a stochastic approximation algorithm of the recursive-least-squares type. The identification process is carried out in two steps: First, the periodic component is eliminated from the load data, and the algorithm is applied to identify the parameters of the residual component; secondly, by expressing the periodic component in terms of load data and its residual component, the same algorithm is applied to identify the coefficients of the Fourier series, equation (3.4).

The identification was performed on Hydro Quebec data, con-

sisting of the load and temperature, measured every hour during a period of three weeks in January of 1972 from Tuesday through Friday. Thus a total of 288 sets of measurements were obtained.

The software was written in FORTRAN on a CDC6200 and the computer storage requirements were varied from 12K to 16K words. The CPU time required for load data identification (23 parameters), was 35 seconds.

3.2.1 Model Parameters and Its Performance

In table 3.1, the parameter values for both the periodic and residual components are displayed. The parameters of the periodic component show that six harmonics are used in the Fourier series (3.4). The parameters of the residual component show that: (i) subsystem B is of second order, since there are two coefficients a_1 and a_2; (ii) the effect of the temperature function U(t) on the load is spread out over 7 hours, through the b_1 to b_7 coefficients, and (iii) the colored noise e(t) affecting the system is correlated with itself for a period of two hours, through the c_1 and c_2 coefficients. Once the coefficients are substituted into equations (3.4) and (3.13), the description of the model is complete, and one can evaluate the performance of the discrete model. This was done by Koutchouk and Panuska.[27] For completeness, some of their results are included in this section, in the form of computer outputs.

Figure 3.4 shows the Hydro Quebec data used. The temperature function U(t) is shown in Fig. 3.4a and the measured load data in Fig. 3.4b. The load is measured in MW, at hourly intervals during the 12 days,

TABLE 3.1

MODEL PARAMETERS

PARAMETERS OF THE PERIODIC COMPONENT $Y_p(t)$						
Constant	$d_0 = 7366$					
Sine Coefficients	$d_1 = -948$	$d_2 = -392$	$d_3 = 100$	$d_4 = -50$	$d_5 = -18$	$d_6 = -26$
Cosine Coefficients	$d_7 = -273$	$d_8 = -199$	$d_9 = -182$	$d_{10} = 200$	$d_{11} = 112$	$d_{12} = -87$

PARAMETERS OF THE RESIDUAL COMPONENT $Y_r(t)$						
a Coefficients	$a_1 = -1.45$			$a_2 = 0.55$		
b Coefficients	$b_1 = 0$	$b_2 = 0$	$b_3 = 0$	$b_4 = 0$	$b_5 = 0$	$b_6 = 3.27$ $b_7 = 2.05$
c Coefficients	$c_1 = -0.82$			$c_2 = 0.15$		

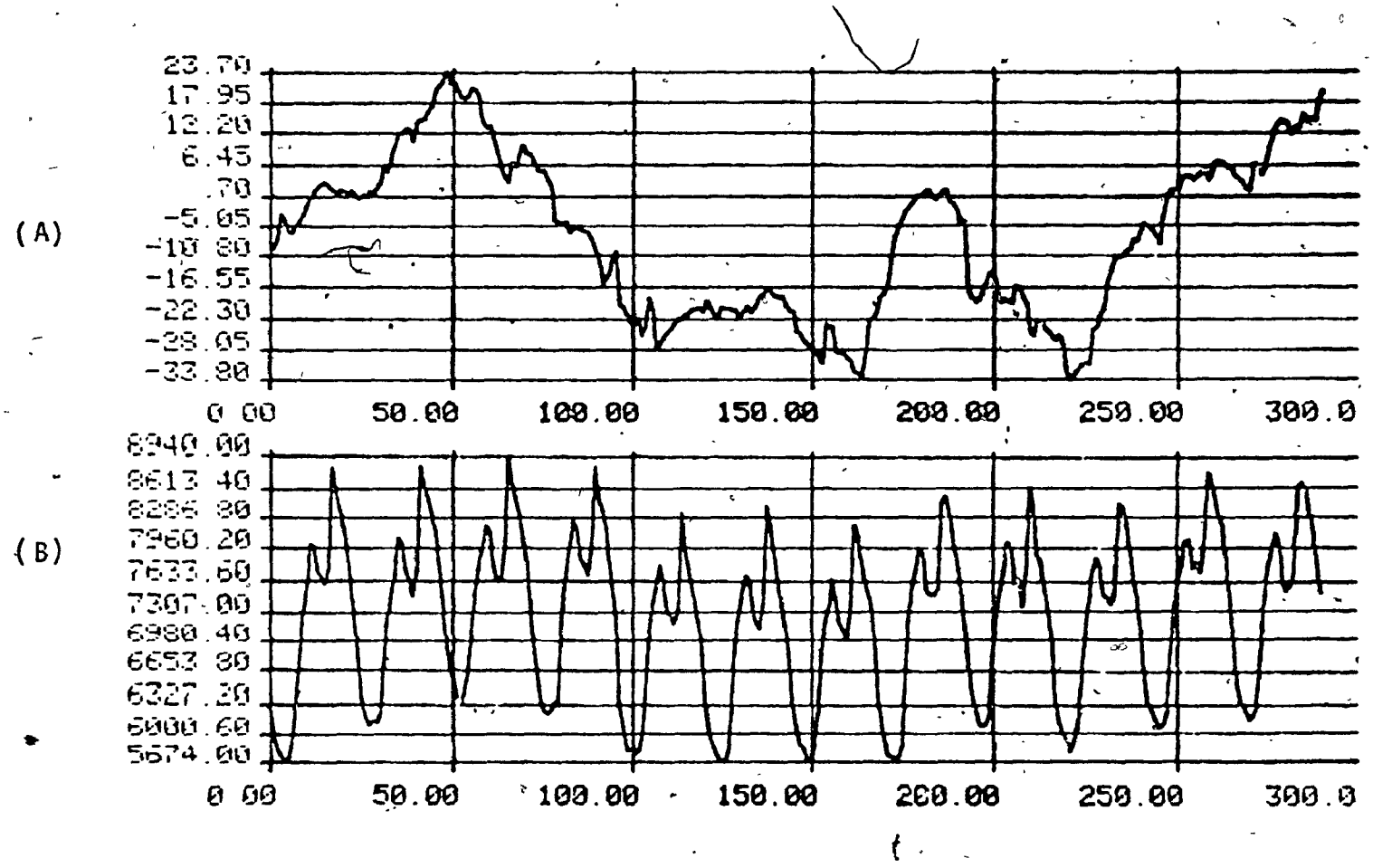

FIG. 3.4 - DATA FILE. A) TEMPERATURE FUNCTION U(T), B) LOAD Z(T)

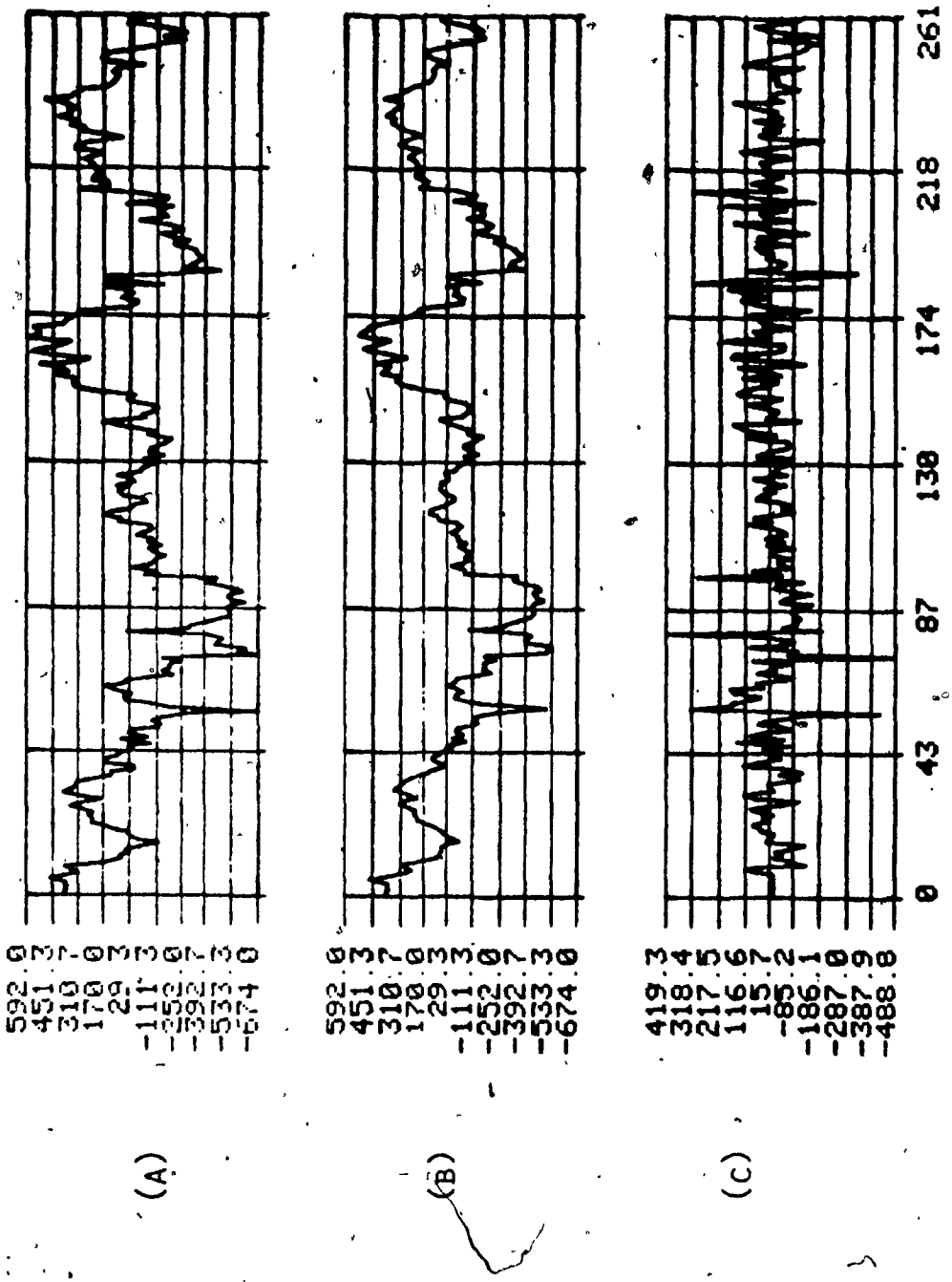

FIG. 3.5 - DISCRETE RESIDUAL COMPONENT $Y_r(t)$. A) ACTUAL
B) SIMULATED C) ERROR

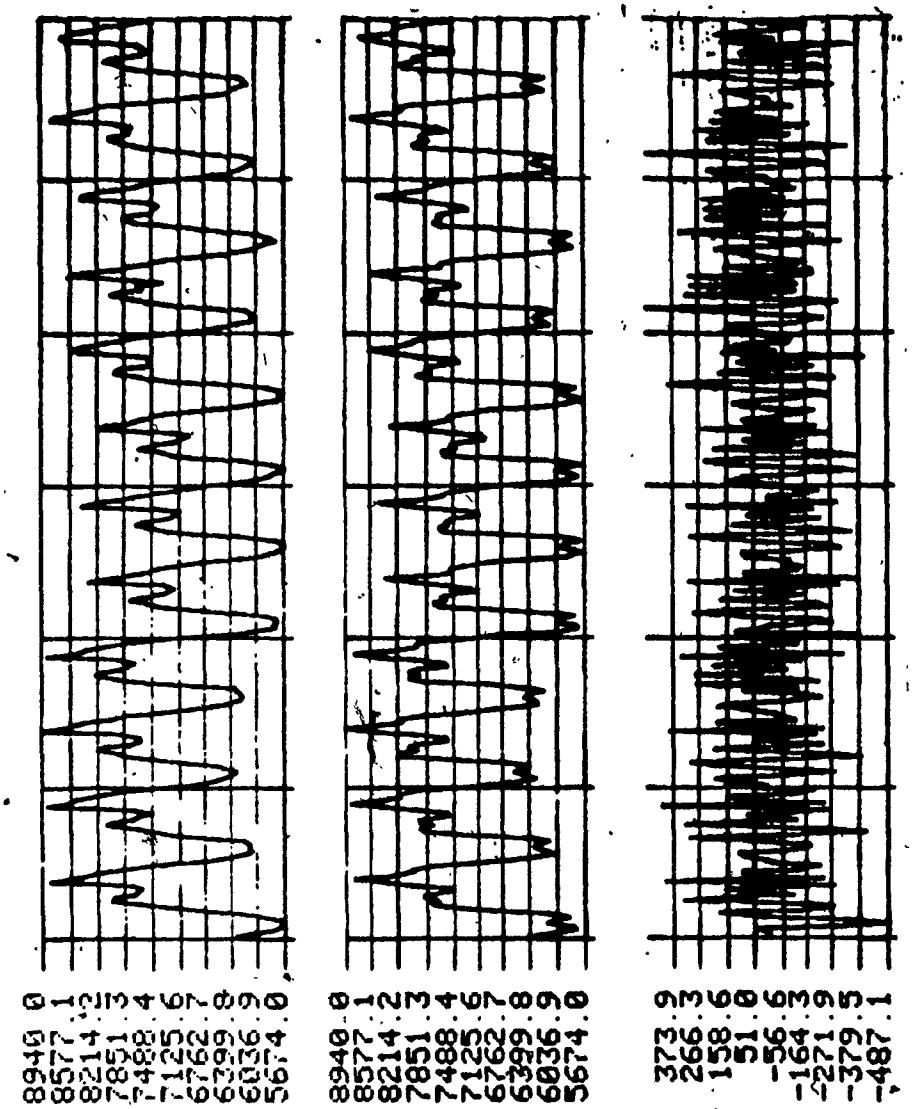

FIG. 3.6 - DISCRETE MODEL PERFORMANCE A) ACTUAL B) SIMULATED C) ERROR

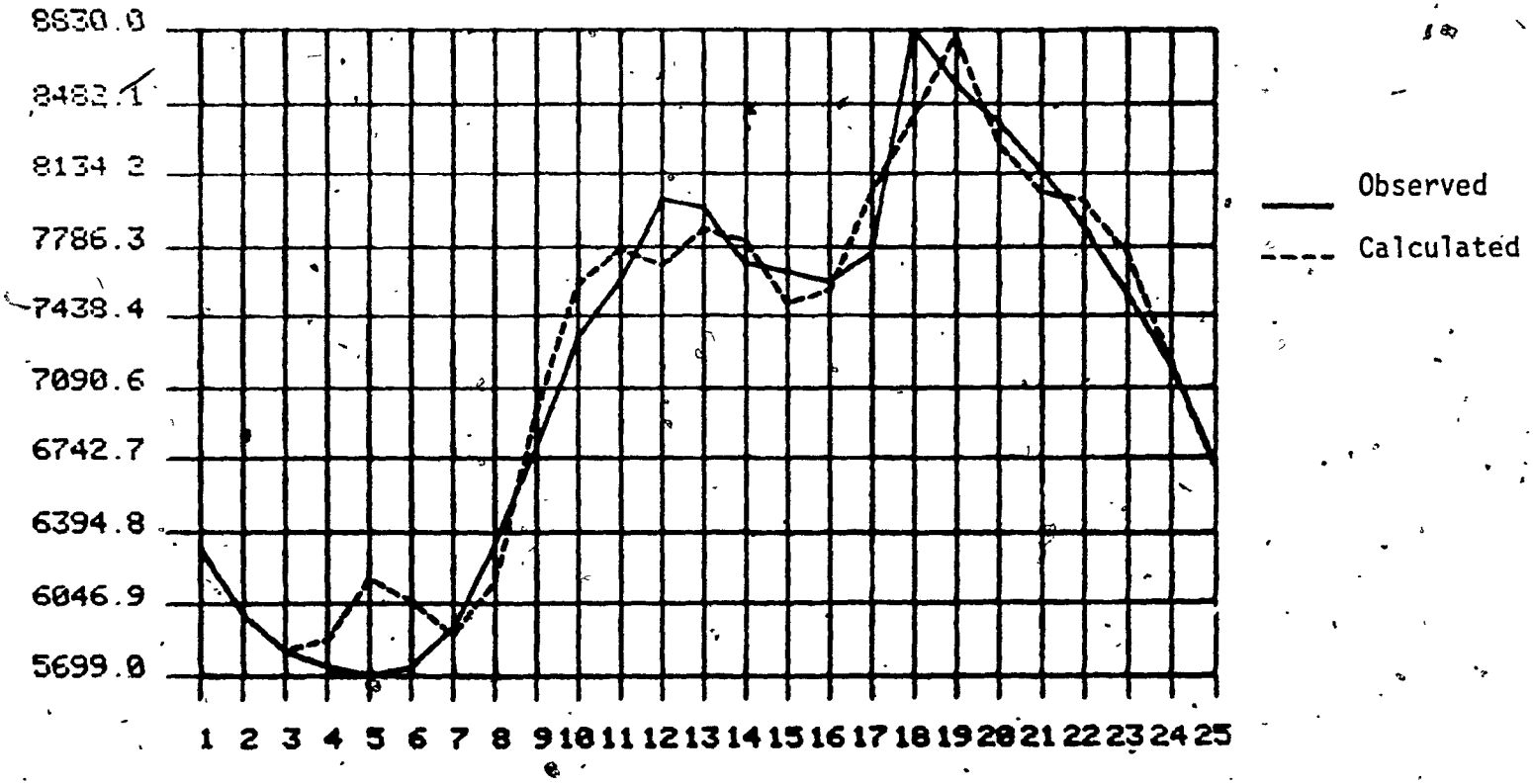

FIG. 3.7 - MODEL PERFORMANCE DURING THE FIRST DAY OF SIMULATION.

while U(t) is given in degrees Farhenhite. The residual component of the load data is shown in Figure 3.5, a. This curve is the residual load after the periodic part of the load data has been removed. The simulated residual load component is shown in Figure 3.5, b, while the error resulting from the simulation of the residual component is shown in Figure 3.5, c. The performance of the model is shown in Figure 3.6. In Figures 3.6, a and b the actual load data and the simulated load are shown respectively. Figure 3.6, c shows the discrepancies of the model from the actual process. The error is sufficiently small at all times, except at the load peaks where its magnitude reaches about 3% to 4% of the total load. A typical daily load model performance is shown in Figure 3.7. It is for the first day of prediction and in general the same kind of errors are observed throughout the forecasting period.

CHAPTER 4
SIMULATION

In this study, we choose to use a hybrid computer for simulating the load model, for the following reasons:

1) To utilize analog components whose dynamics resemble those of real systems.
2) To combine the speed of the analog computer with the accuracy of the digital computer.
3) To permit processing of incoming data which are partially discrete and partially continuous.
4) To increase the flexibility of analog computation by using digital memory and control.
5) The load peaks are the most interesting parts in any forecast, hence the model must follow the load peaks accurately enough during the whole peak period. Simulation of the model in discrete time does not allow us to evaluate the model's performance at the load peaks, while hybrid simulation does.

4.1 Transformation from Discrete to Analog Model

In hybrid simulation, the analog computer is used to simulate the model dynamics, while the digital computer provides precision and repeatability of the simulation. Since the analog computer simulates quantities continuously in time, it is necessary for the model being simulated to be described by equations that are also continuous in time.

The simulated load consists of two components $Y_p(t)$ and $Y_r(t)$, of which $Y_p(t)$ is a Fourier series and is hence described continuously in time. Therefore, only the description of the residual component $Y_r(t)$ needs to be transformed from discrete-time to continuous-time.

The component $Y_r(t)$ is described by a difference equation, which is to be transformed into a differential equation. This is achieved in three steps:

(i) Transformation of difference equation to z-domain transfer functions.

(ii) Transformation of transfer functions from z-domain to s-domain, and

(iii) Transformation from s-domain transfer functions to continuous-time differential equation.

(i) TRANSFORMATION OF DIFFERENCE EQUATION TO z-DOMAIN TRANSFER FUNCTIONS

The residual component $Y_r(t)$ is governed by

$$Y_r(nT) = 1.45\,Y_r(nT-T) - 0.55\,Y_r(nT-T) + 3.27\,U(nT-6T) + 2.05\,U(nT-7T) + W(nT) - 0.82\,W(nT-T) + 0.15\,W(nT-2T) \quad (4.1)$$

Taking z-transforms of both sides of (4.1) gives

$$\tilde{Y}_r(z) = 1.45z^{-1}\tilde{Y}_r(z) - 0.55z^{-2}\tilde{Y}_r(z) + 3.27z^{-6}\tilde{U}(z) + 2.05z^{-7}\tilde{U}(z) + \tilde{W}(z) - 0.82z^{-1}\tilde{W}(z) + 0.15z^{-2}\tilde{W}(z) \quad (4.2)$$

or, rearranging terms,

$$(1 - 1.45z^{-1} + .55z^{-2})\tilde{Y}_r(z) = (3.27 - 2.05z^{-1})z^{-6}\tilde{U}(z) + (1 - .82z^{-1} + .15z^{-2})\tilde{W}(z) \quad (4.3)$$

Solving for $\tilde{Y}_r(z)$, we obtain

$$\tilde{Y}_r(z) = \frac{(3.27 - 2.05z^{-1})z^{-6}}{1 - 1.45z^{-1} + .55z^{-2}} \tilde{U}(z) + \frac{1 - .82z^{-1} + .15z^{-2}}{1 - 1.45z^{-1} + .55z^{-2}} \tilde{W}(z) \qquad (4.4)$$

or

$$\tilde{Y}_r(z) = \frac{(3.27z^2 - 2.05z)z^{-6}}{z^2 - 1.45z + .55} \tilde{U}(z) + \frac{z^2 - .82z + .15}{z^2 - 1.45z + .55} \tilde{W}(z) \qquad (4.5)$$

Defining:

$$\tilde{F}_1(z) = \frac{3.27z^2 - 2.05z}{z^2 - 1.45z + .55} \qquad (4.6)$$

$$\tilde{F}_2(z) = \frac{z^2 - .82z + .15}{z^2 - 1.45z + .55} \qquad (4.7)$$

$$\tilde{V}(z) = z^{-6} \tilde{U}(z) \qquad (4.8)$$

We can write

$$\tilde{Y}_r(z) = \tilde{F}_1(z) \cdot \tilde{V}(z) + \tilde{F}_2(z) \cdot \tilde{W}(z) \qquad (4.9)$$

The block diagram of Figure 4.1 shows the modelling of the residual component, in terms of z-domain transfer functions, as given by (4.9).

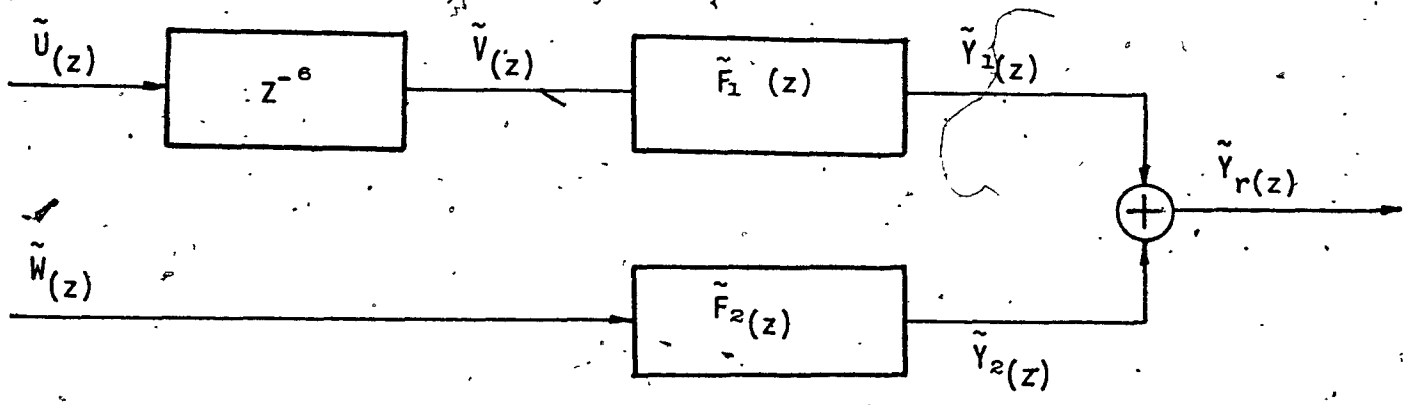

FIG. 4.1 - BLOCK DIAGRAM MODELLING THE RESIDUAL COMPONENT $\tilde{Y}_r(z)$.

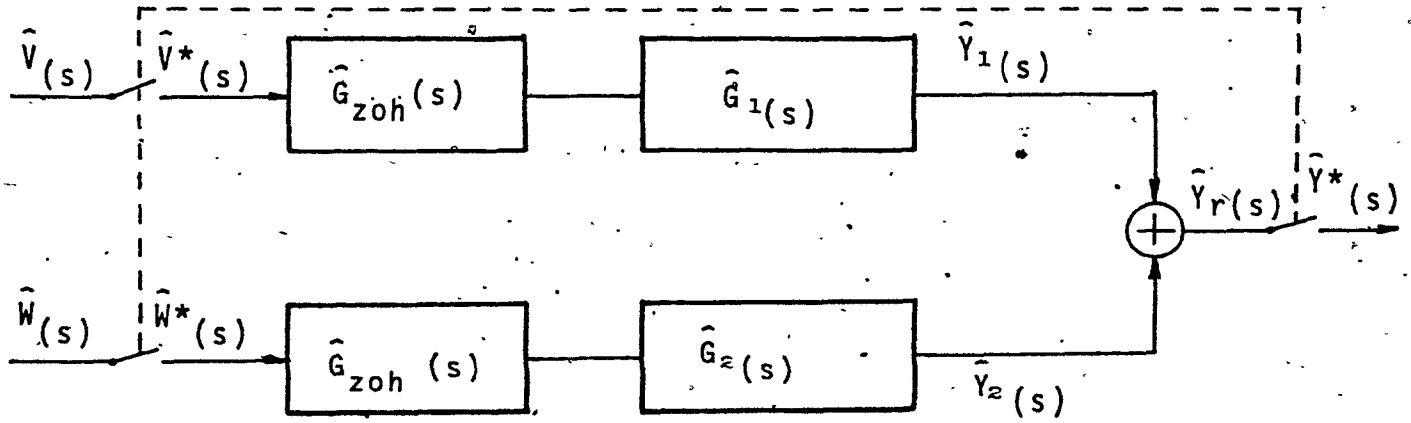

FIG. 4.2 - BLOCK DIAGRAM MODELLING THE RESIDUAL COMPONENT $\hat{Y}_r(s)$

(ii) TRANSFORMATION OF TRANSFER FUNCTIONS FROM z-DOMAIN TO s-DOMAIN

Next, we transform the z-domain transfer functions to s-domain transfer functions, which consist of a zero-order hold followed by another transfer function. This situation is depicted in Fig. 4.2. The transfer function of the zero-order hold network in the s-domain is given by

$$\hat{G}_{zoh}(s) = \frac{1 - e^{-st}}{s} \tag{4.10}$$

The following symbols are now adopted in order to simplify the analysis.

$L_z \left\{ \hat{H}(s) \right\}$ denotes the z-transform equivalent of $\hat{H}(s)$, and

$L_s \left\{ \tilde{H}(z) \right\}$ denotes the s-transform equivalent of $\tilde{H}(z)$.

From the block diagram of figure 4.2, the following relationship can be readily written:

$$\frac{\hat{Y}_1(s)}{\hat{V}^*(s)} = \hat{G}_{zoh}(s) \cdot \hat{G}_1(s) \tag{4.11}$$

Taking the z-transform of both sides of (4.11) gives

$$\frac{\tilde{Y}_1(z)}{V(z)} = L_z \left\{ \hat{G}_{zoh}(s) \cdot \hat{G}(s) \right\} \tag{4.12}$$

or, $$\tilde{F}_1(z) = L_z \left\{ \frac{1 - e^{-st}}{s} \cdot \hat{G}(s) \right\} \tag{4.13}$$

where $\tilde{F}_1(z)$ is defined in (4.6).

Substituting $z = e^{st}$ in equation (4.13) yields

$$\tilde{F}_1(z) = (1 - z^{-1}) L_z \left\{ \frac{\hat{G}_1(s)}{s} \right\} \tag{4.14}$$

or

$$L_z \left\{ \frac{\hat{G}_1(s)}{s} \right\} = \tilde{F}_1(z) \cdot \frac{z}{z - 1} \tag{4.15}$$

An equivalent form of (4.15) is

$$\frac{\hat{G}_1(s)}{s} = L_s \left\{ \tilde{F}_1(z) \cdot \frac{z}{z-1} \right\} \tag{4.16}$$

Substituting for $\tilde{F}_1(z)$ from (4.6), we obtain

$$\frac{\hat{G}_1(s)}{s} = L_s \left\{ \frac{3.27z^2 - 2.05z}{z^2 - 1.45z + .55} \cdot \frac{z}{z-1} \right\} \tag{4.17}$$

To find the desired s-domain equivalent, we expand the expression in the brackets of equation (4.17) into partial fractions. This gives

$$\frac{(3.27z^2 - 2.05z)z}{(z^2 - 1.45z + .55)(z - 1)} = \frac{12.37z}{z - 1} - \frac{9.1z^2 + 6.17z}{z^2 - 1.45z + .55} \qquad (4.18)$$

therefore

$$\frac{\hat{G}_1(s)}{s} = L_s \left\{ 12.37 \frac{z}{z - 1} - 9.1 \frac{z^2 - .725z}{z^2 - 1.45z + .55} \right\} \qquad (4.19)$$

Since,

$$L_s \left\{ \frac{z}{z - 1} \right\} = \frac{1}{s} \qquad (4.20)$$

and

$$L_s \left\{ \frac{z^2 - ze^{-aT}\cos\omega_o T}{z^2 - 2ze^{-aT}\cos\omega_o T + e^{-2at}} \right\} = \frac{s + a}{(s+a)^2 + \omega_o^2} \qquad (4.21)$$

we have from equation (4.19)

$$\frac{\hat{G}_1(s)}{s} = 12.37 \frac{1}{s} - 9.1 \frac{s + a}{(s+a)^2 + \omega_o^2} \qquad (4.22)$$

where,

$$e^{-aT} = 0.7416 \implies aT = 0.3$$

and

$$\cos\omega_o T = 0.9776 \implies \omega_o T = 12.15^{\circ} = 0.2119 \text{ rad.}$$

The sampling period is one hour, i.e. 3600 sec. Hence,

$$a = \frac{0.3}{3600} = 8.333 \times 10^{-5} \text{ sec}^{-1}$$

and

$$\omega_o = \frac{0.2119}{3600} = 5.886 \times 10^{-5} \text{ rad/sec}$$

Substitution of the above values into equation (4.22) yields,

$$\frac{\hat{G}_1(s)}{s} = \frac{3.27\ s^2 + 130.328 \times 10^{-5}s + 1287.494 \times 10^{-10}}{s(s^2 + 16.666 \times 10^{-5}s + 104.082 \times 10^{-10})} \qquad (4.23)$$

therefore,

$$\hat{G}_1(s) = \frac{3.27s^2 + 130.328 \times 10^{-5}s + 1287.494 \times 10^{-10}}{s^2 + 16.666 \times 10^{-5}s + 104.082 \times 10^{-10}} \qquad (4.24)$$

Similarly, the transfer function $\hat{G}_2(s)$ can be found to be

$$\hat{G}_2(s) = \frac{s^2 + 35.832 \times 10^{-5}s + 343.470 \times 10^{-10}}{s^2 + 16.666 \times 10^{-5}s + 104.082 \times 10^{-10}} \qquad (4.25)$$

iii) TRANSFORMATION FROM s-DOMAIN TRANSFER FUNCTIONS TO CONTINUOUS TIME DIFFERENTIAL EQUATION

The residual component $\hat{Y}_r(s)$ is related to $\hat{V}(s)$ and $\hat{W}(s)$ by

$$\hat{Y}_r(s) = \frac{3.27s^2 + 130.328 \times 10^{-5}s + 1287.494 \times 10^{-10}}{s^2 + 16.666 \times 10^{-5}s + 104.082 \times 10^{-10}} \hat{V}(s) + \frac{s^2 + 35.832 \times 10^{-5}s + 343.470 \times 10^{-10}}{s^2 + 16.666 \times 10^{-5}s + 104.082 \times 10^{-10}} \hat{W}(s) \qquad (4.26)$$

$$\text{or} \quad (s^2 + 16.666 \times 10^{-5}s + 104.082 \times 10^{-10})\hat{Y}_r(s) =$$

$$(3.27s^2 + 130.328 \times 10^{-5}s + 1287.494 \times 10^{-10})\,\hat{V}(s) + \qquad (4.27)$$

$$(s^2 + 35.832 \times 10^{-5}s + 343.470 \times 10^{-10})\,\hat{W}(s)$$

In the time domain, (4.27) is equivalent to the sought differential equation

$$\ddot{Y}_r(t) + 16.666 \times 10^{-5}\dot{Y}_r(t) + 104.082 \times 10^{-10}Y_r(t) =$$

$$3.27\,\ddot{V}(t) + 130.328 \times 10^{-5}\dot{V}(t) + 1287.494 \times 10^{-10}V(t) + \qquad (4.28)$$

$$\ddot{W}(t) + 35.832 \times 10^{-5}\dot{W}(t) + 343.470 \times 10^{-10}W(t)$$

4.2 Hybrid Computer Implementation

The hybrid computing facility used in this simulation is a "true hybrid" system, the EAI 690. The 690 system consists of an EAI 640 digital computer, interfaced to an EAI 680 analog computer by an EAI 693 hybrid interface unit.

4.2.1 Analog Implementation

The implementation on the analog computer includes the programming of the two components of the model, $Y_p(t)$ and $Y_r(t)$, and their sum, which gives the simulated load. The two steps preceeding the analog implementation are: (i) time scaling, which is needed to speed up the simulation, and (ii) amplitude scaling, which is needed in order to avoid overloading of the analog computer components.

(i) TIME SCALING

It is desired to speed up the performance of the model, so that its simulation is achieved in seconds, instead of 12 days which is the period of the actual process. We choose to supply the hourly data to the model every 2 sec. Therefore, the length of the simulation becomes 288 x 2 = 576 sec, instead of 288 hours or 1036800 sec. This choice defines the time scale factor α, as

$$\alpha = \frac{576}{1036800} = 55.55 \times 10^{-5} \qquad (4.29)$$

A further speed up of the simulation by a factor of 10 is done via the time scale controls available on the analog console. The choice of "F SEC" (Fast Seconds) achieves this speed-up, thus avoiding the use of a large time-scale factor.

After time scaling the fundamental frequency ω of the Fourier series (3.4) defining the periodic component $Y_p(t)$ becomes

$$\omega_s = \frac{2\pi}{24 \times 3600 \times \alpha} = \frac{2\pi}{86400 \times 55.55 \times 10^{-5}} = 0.1308 \text{ rad/sec} \qquad (4.30)$$

Therefore the higher harmonies of the Fourier series are

$$\begin{aligned} 2\,\omega_s &= 0.2617 \quad \text{rad/sec} \\ 3\,\omega_s &= 0.3925 \quad \text{rad/sec} \\ 4\,\omega_s &= 0.5233 \quad \text{rad/sec} \\ 5\,\omega_s &= 0.6542 \quad \text{rad/sec} \\ 6\,\omega_s &= 0.7850 \quad \text{rad/sec} \end{aligned} \qquad (4.31)$$

In order to time scale the residual component $Y_r(t)$, we make the transformation

$$f\left(\frac{t}{\alpha}\right) \longrightarrow f(t) \tag{4.32}$$

in the equation (4.28), which after the necessary algebra takes the form

$$\begin{aligned} &\ddot{Y}_r(t) + \frac{16.666 \times 10^{-5}}{\alpha}\dot{Y}_r(t) + \frac{104.082 \times 10^{-10}}{\alpha^2} Y_r(t) = \\ &3.27\,\ddot{V}(t) + \frac{130.328 \times 10^{-5}}{\alpha}\dot{V}(t) + \frac{1287.494 \times 10^{-10}}{\alpha^2} V(t) + \\ &\ddot{W}(t) + \frac{35.832 \times 10^{-5}}{\alpha}\dot{W}(t) + \frac{343.470 \times 10^{-10}}{\alpha^2} W(t) \end{aligned} \tag{4.33}$$

Substituting for α, we obtain the time scaled differential equation for the residual component:

$$\begin{aligned} &\ddot{Y}_r(t) + 0.3000\,\dot{Y}_r(t) + 0.0337\,Y_r(t) = \\ &3.27\,\ddot{V}(t) + 2.3460\,\dot{V}(t) + 0.4171\,V(t) + \\ &\ddot{W}(t) + 0.6450\,\dot{W}(t) + 0.1112\,W(t) \end{aligned} \tag{4.34}$$

(ii) AMPLITUDE SCALING

The components of the EAI 680 analog computer can operate in the range ±1 unit without being overloaded. This dictates an amplitude

scale factor β, which reduces the amplitude of the signals accordingly. In our case we choose

$$\beta = 9480 \tag{4.35}$$

The periodic component, $Y_p(t)$, contains a constant term $d_o = 7366$ which does not provide any important information. This term is subtracted from the periodic component $Y_p(t)$, which after time and amplitude scaling becomes

$$X_p(t) = \frac{Y_p(t) - 7366}{\beta} \tag{4.36}$$

or

$$\begin{aligned} X_p(t) = {} & -0.100 \sin\omega_s t - 0.0413 \sin 2\omega_s t + 0.0105 \sin 3\omega_s t \\ & -0.0052 \sin 4\omega_s t - 0.0018 \sin 5\omega_s t - 0.0027 \sin 6\omega_s t \\ & -0.0287 \cos\omega_s t + 0.0209 \cos 2\omega_s t - 0.0191 \cos 3\omega_s t \\ & +0.0210 \cos 4\omega_s t + 0.0118 \cos 5\omega_s t - 0.0091 \cos 6\omega_s t \end{aligned} \tag{4.37}$$

To amplitude scale the residual component $Y_r(t)$, we first define

$$X_r(t) = \frac{Y_r(t)}{\beta} \tag{4.38}$$

$$S(t) = \frac{W(t)}{\beta} \tag{4.39}$$

and

$$R(t) = \frac{3.27 \times V(t)}{\beta} \tag{4.40}$$

Substitution of (4.38) through (4.40) into (4.34) results in the time

and amplitude scaled differential equation for the residual component:

$$\ddot{X}_r(t) + 0.3000\,\dot{X}_r(t) + 0.0337\,X_r(t) = \ddot{R}(t) + 0.9240\,\dot{R}(t) + 0.1275\,R(t) + \ddot{S}(t) + 0.6450\,\dot{S}(t) + 0.1112\,S(t) \qquad (4.41)$$

The programming of the Fourier series (4.37) is based on the solution of the differential equation,

$$\ddot{x}(t) + \omega^2 x(t) = 0 \qquad (4.42)$$

which is given by

$$x(t) = a\cos\omega t - b\sin\omega t \qquad (4.43)$$

Therefore the basic circuit for generating a sinusoidal waveform is the analog implenentation of (4.42). Figure 4.3 shows this implementation. The values of the potentiometers p_0 correspond to the generated frequency ω, while the values of p_1 and p_2 supply the coefficient values a and b respectively. The overall programming of (4.37) generates the periodic component $X_p(t)$, as shown in Figure 4.4. Programming of the differential equation (4.41) results in the residual component $X_r(t)$. This is shown in Figure 4.5. Summation of the periodic and residual components as shown in Figure 4.6, results in the generated normalized load Q(t), which is given by

$$Q(t) = X_p(t) + X_r(t) \qquad (4.45)$$

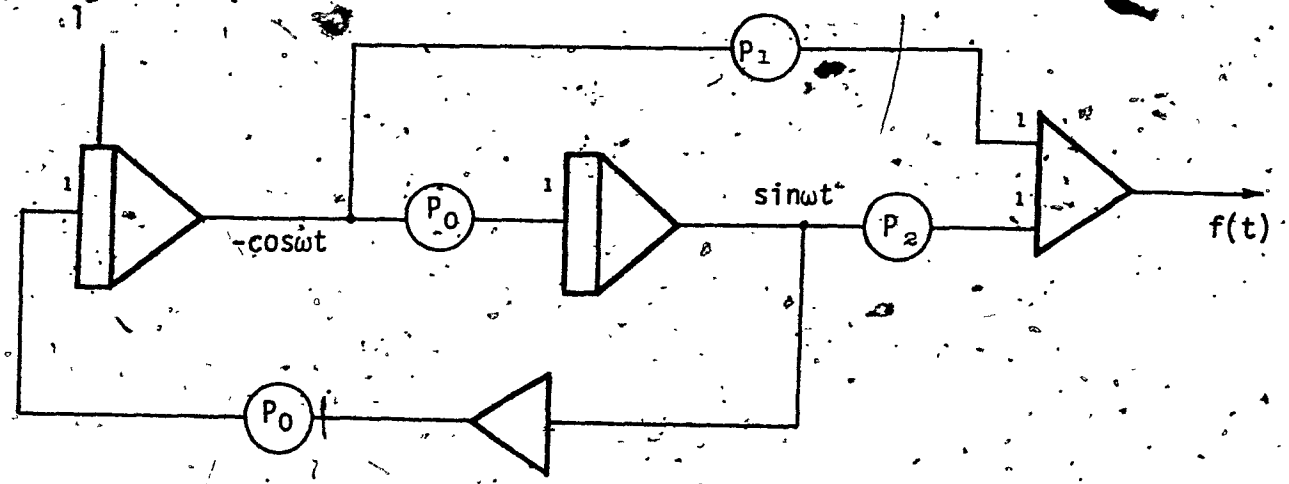

FIG. 4.3 GENERATION OF THE SINUSOIDAL WAVEFORM f(t)

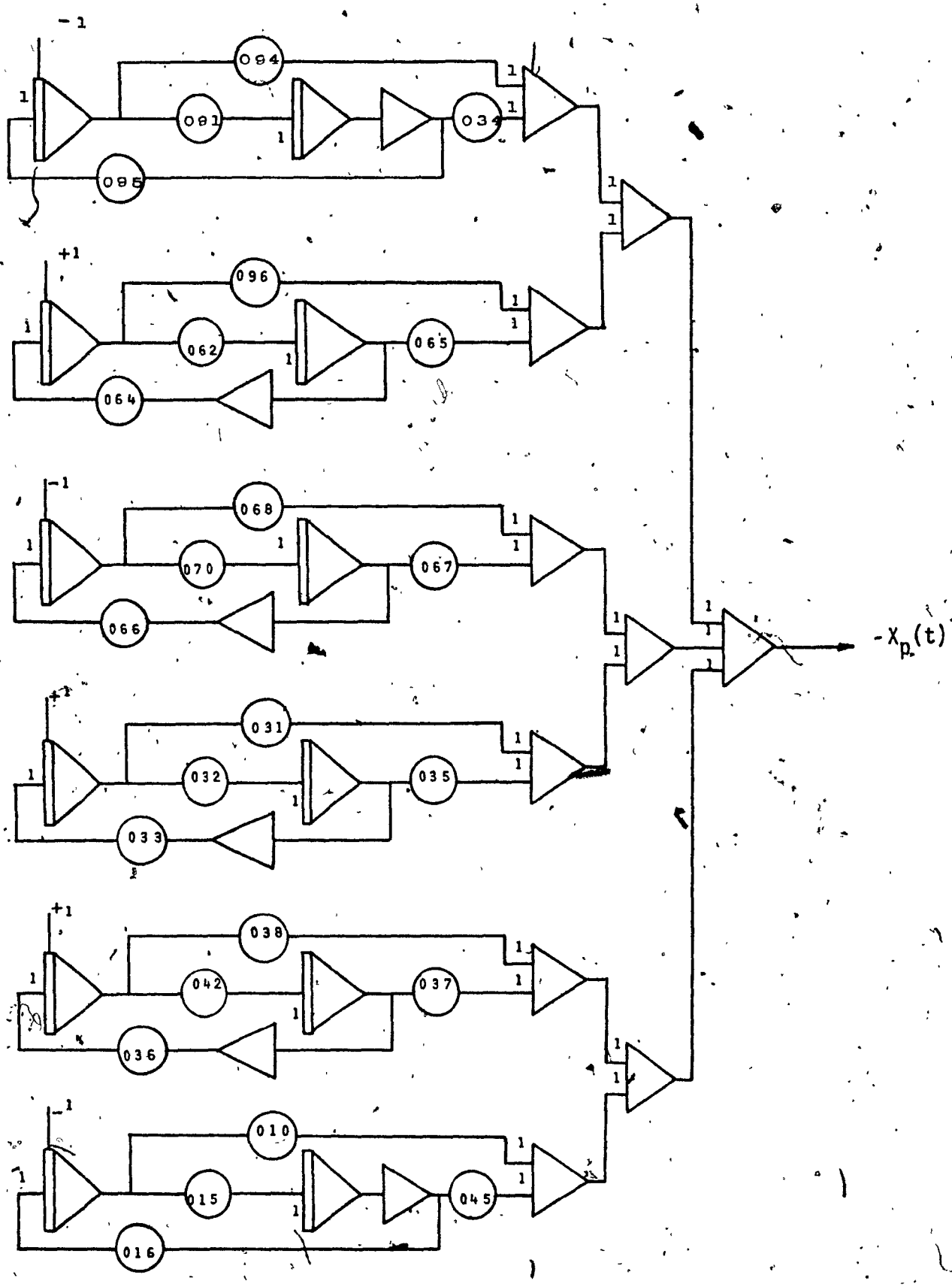

FIG. 4.4 - ANALOG PROGRAMMING OF PERIODIC COMPONENT $X_p(t)$

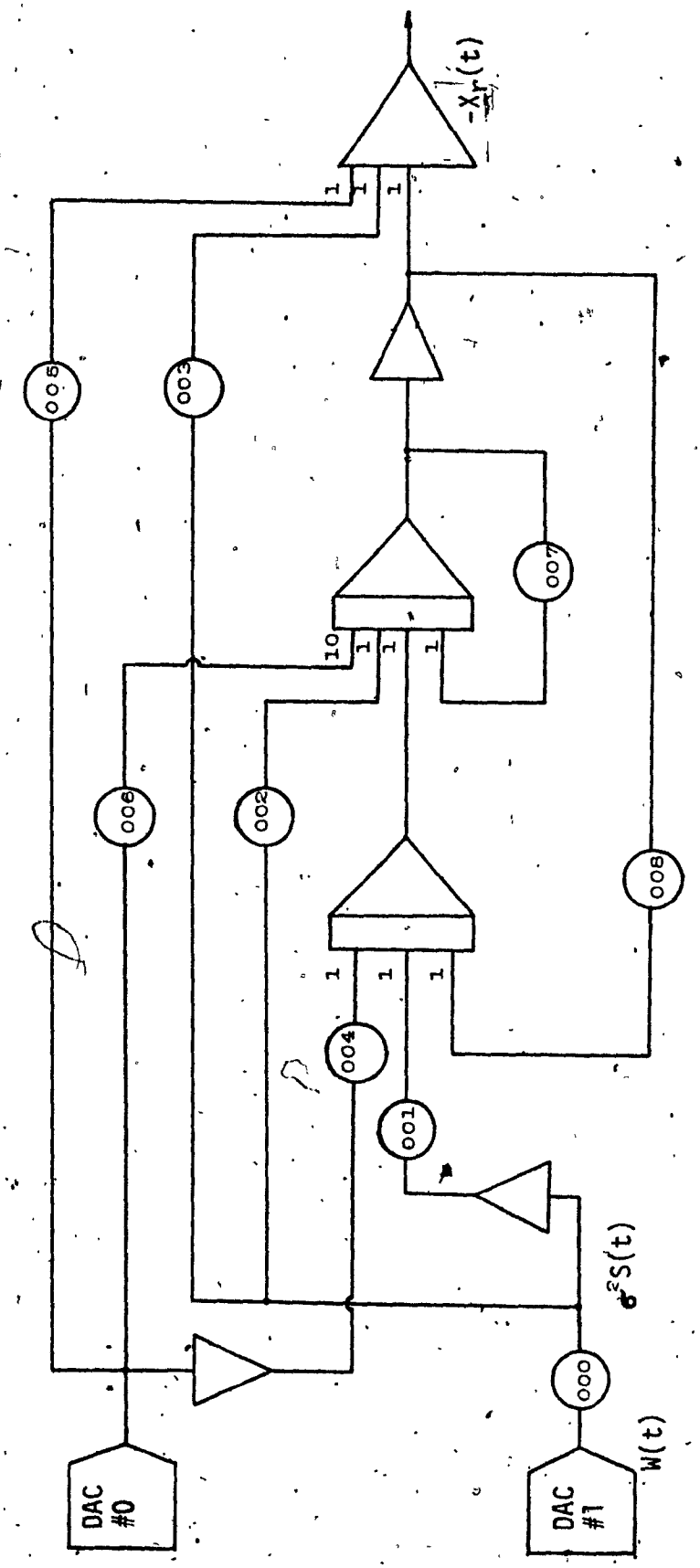

FIG. 4.5 - ANALOG PROGRAMMING OF RESIDUAL COMPONENT $x_r(t)$

TABLE 4.1

POTENTIOMETERS AND THEIR VALUES

NO.	POTENTIOMETER	VALUE	NO.	POTENTIOMETER	VALUE
1	000	0.0105*	18	036	0.6542
2	001	0.1112	19	037	0.0018
3	002	0.6450	20	038	0.0118
4	003	1.0000	21	042	0.6542
5	004	0.1275	22	045	0.0027
6	005	1.0000	23	062	0.2617
7	006	0.0924	24	064	0.2617
8	007	0.3000	25	065	0.0413
9	008	0.0337	26	066	0.3925
10	010	0.0091	27	067	0.0105
11	015	0.7850	28	068	0.0191
12	016	0.7850	29	070	0.3925
13	031	0.0210	30	091	0.1308
14	032	0.5233	31	094	0.0287
15	033	0.5233	32	095	0.1308
16	034	0.1000	33	096	0.0209
17	035	0.0052			

* The value of the potentiometer 000 is

$$\frac{\sigma^2}{9480} = \frac{100}{9480} = 0.0105$$

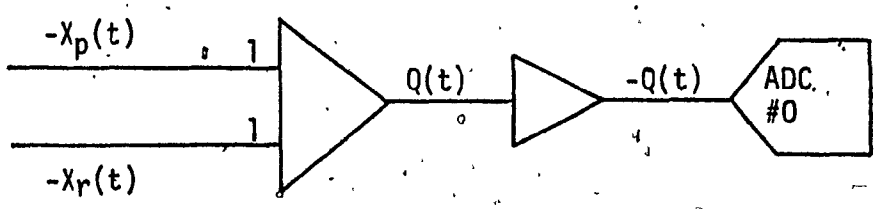

FIG. 4.6 - GENERATION OF NORMALIZED LOAD Q(t)

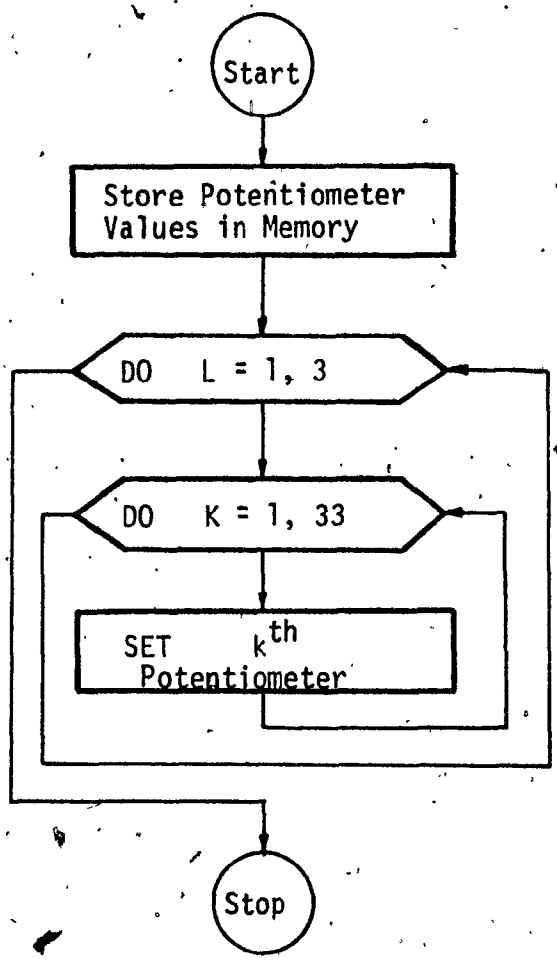

FIGURE 4.7 - PROGRAM POTSET

or $$Q(t) = \frac{Y_p(t) + Y_r(t) - 7366}{9480} \qquad (4.46)$$

The potentiometers used and their corresponding values are shown in Table 4.1.

4.2.2 Digital Implementation

The hybrid oriented software which is designed to perform tasks necessary for the hybrid simulation, constitutes the digital implementation. The software, shown in Appendix A, includes two programs: (i) POTSET, which is used to set the potentiometers, and (ii) HYBSIM, which performs the simulation. By employing this scheme for the software, we avoid unnecessary repetition of the potentiometer settings, thus reducing the computer time used. Furthermore, this scheme provides greater computer storage for the main program HYBSIM. Figures 4.7 and 4.8 show the structure of the POTSET and HYBSIM programs respectively, in the form of flowcharts. As soon as the simulation of the model is performed and simulated load values are stored in memory, the HYBSIM calculates the Average Absolute Error, defined by

$$\text{Average Absolute Error} = \frac{1}{288} \sum_{i=1}^{288} \left| X(i) - Z(i) \right| \qquad (4.47)$$

where $Z(i)$ is the actual load data, and

$$X(i) = 9480 \cdot Q(i) + 7366 \qquad (4.48)$$

This error is considered an overall measure of the model's performance. The values of $U(t)$, $Z(t)$, $X(t)$ and $E(t) = X(t) - Z(t)$ obtained from the simulation are shown in APPENDIX B.

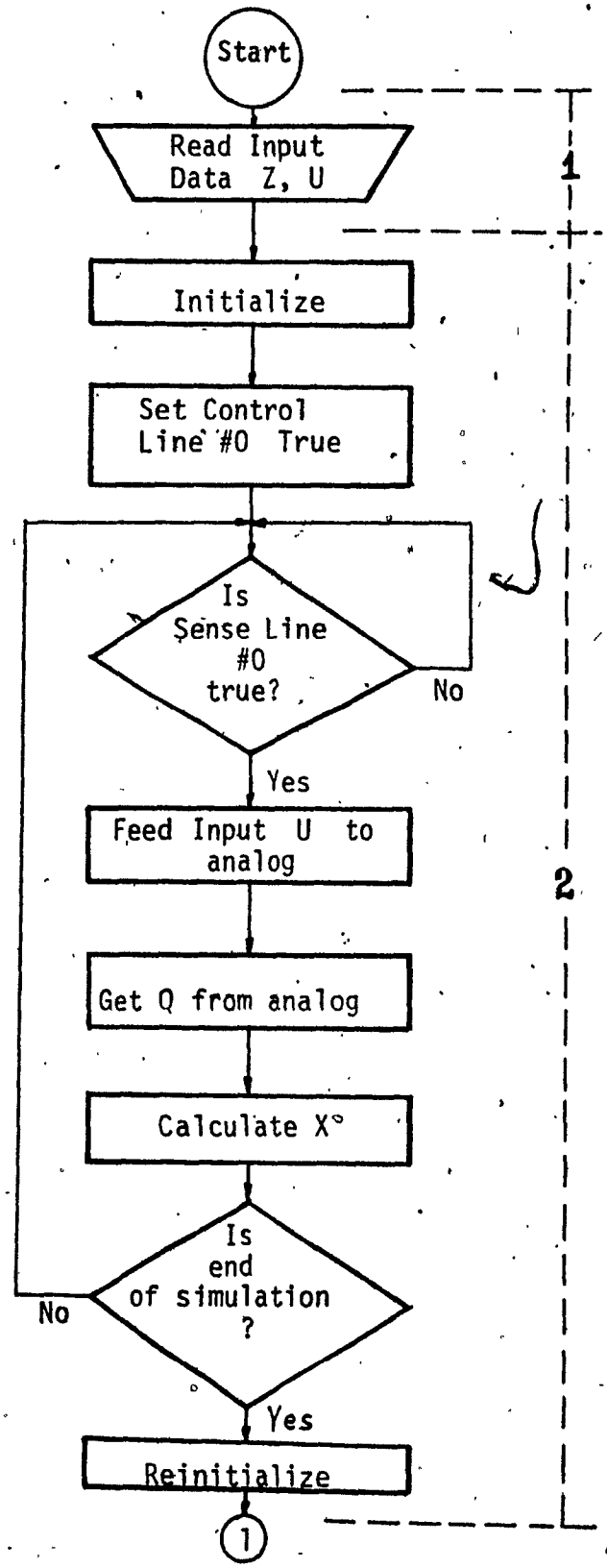

FIGURE 4.8 - PROGRAM HYBSIM (CONTINUED)

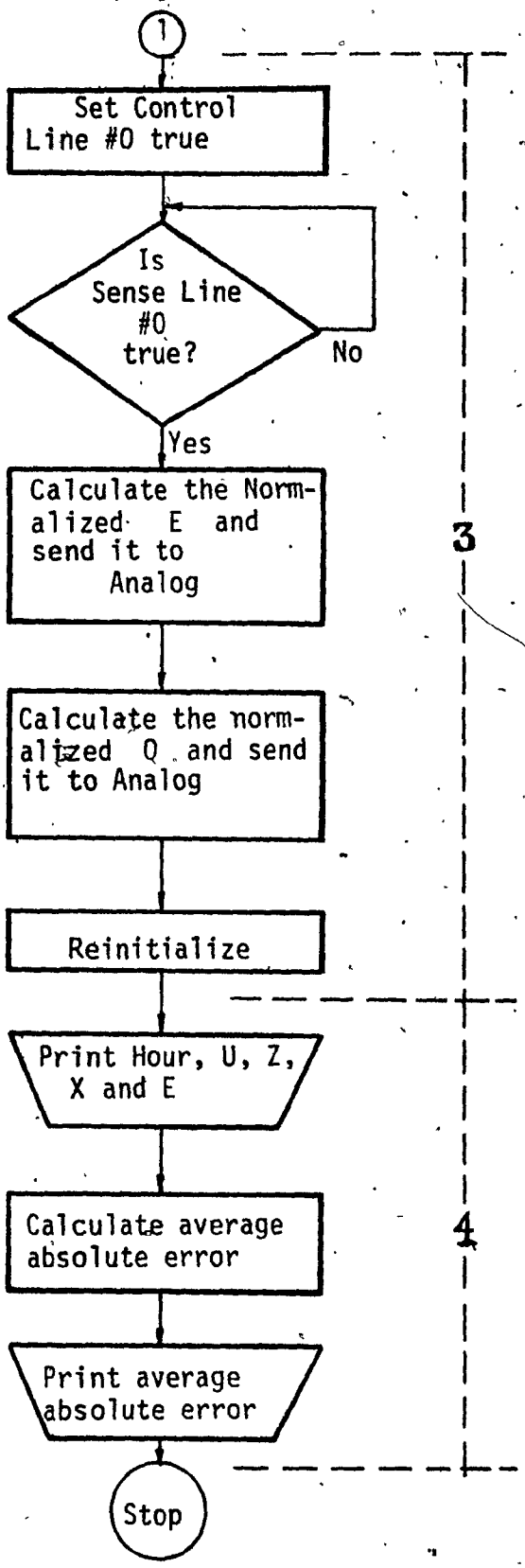

FIG. 4.8 - PROGRAM HYBSIM

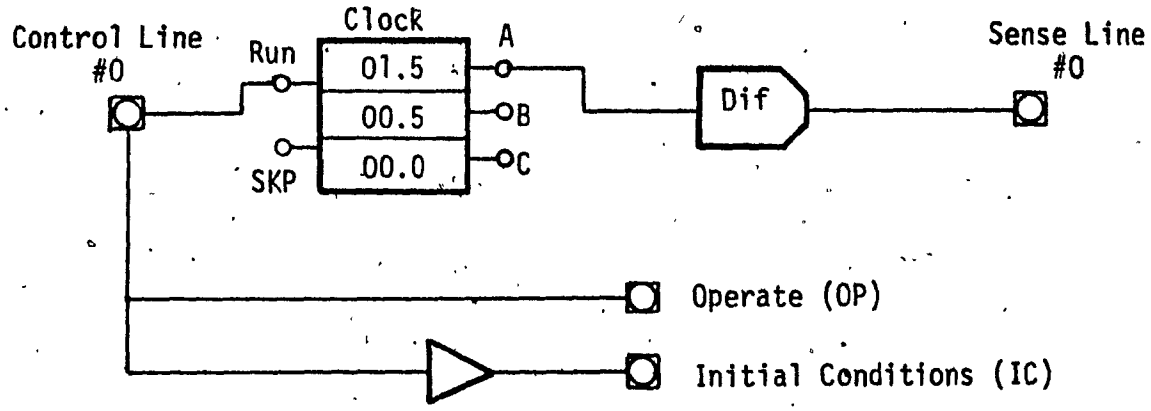

FIG. 4.9 - LOGIC CIRCUIT TO CONTROL INITIAL CONDITIONS, OPERATE MODE AND SAMPLING PERIOD.

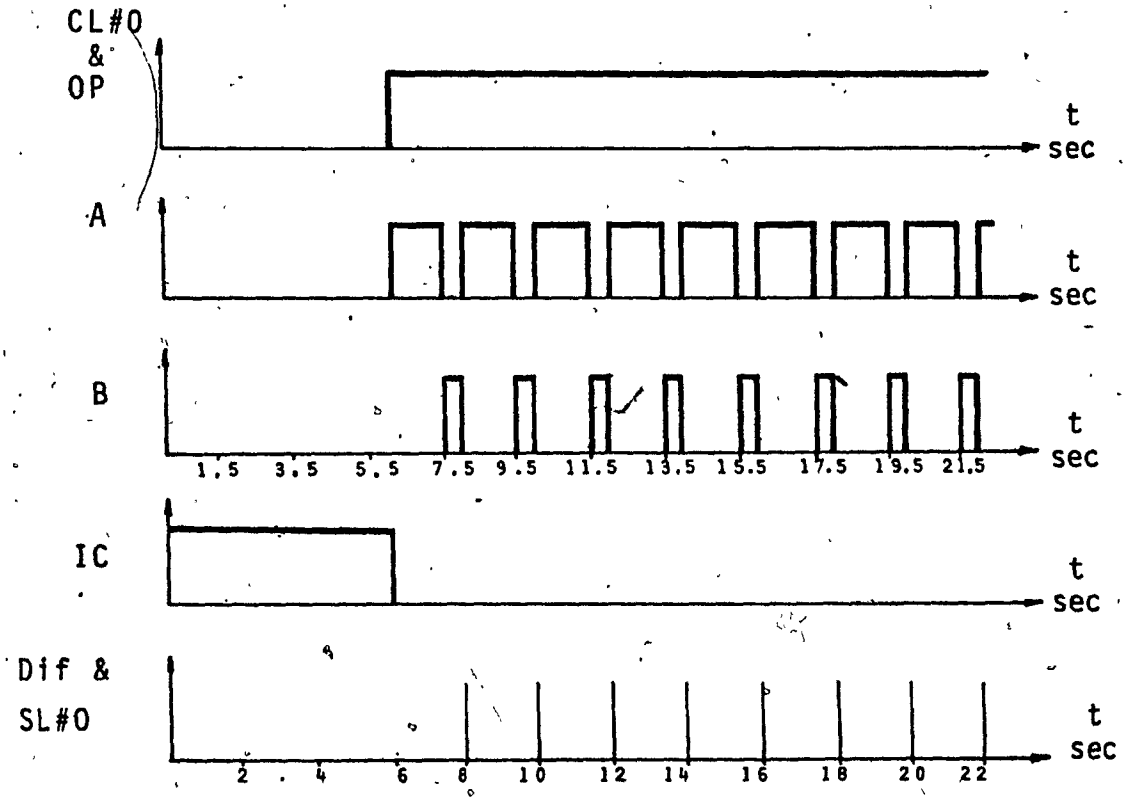

FIG. 4.10 - GENERATED PULSES FROM THE LOGIC CIRCUITS OF FIG. 4.9.

4.2.3 Time Control

The sequential use of Digital to Analog and Analog to Digital converters is based on the operation of the time control area on the analog console. Figure 4.9 shows the implemented logic circuit for the generation of the pulses used to detect the sampling instant. Figure 4.10 shows the pulses generated at the outputs of the counter, the differentiator and the sense line #0. The counter, otherwise known as REP-OP timer, has 2 inputs and 3 outputs. When the input RUN is high the timer generates 100 pulses per second. The output A stays high until 15 pulses (150 msec) have been received, then B will become high for a duration of 5 more pulses (50 msec), while A will be low during this time. The output A of the REP-OP timer is connected to a differentiator which produces an output pulse one clock period long (10 msec) whenever its input changes from 0 to 1. The output of the differentiator is connected to sense line #0, whose status determines the sampling instant.

4.3 Performance of the Model

Simulation of the load model on the EAI 690 hybrid computing system requires two inputs, namely: the temperature dependent function U(t), and a Gaussian noise supplied from an analog noise generator of HEWLETT-PACKARD. The noise bandwidth is 50 KHz. Since there is no theoretical way of obtaining the amplitude and variance of the noise, the simulation was tested for various values, and it was found that an amplitude of 0.4 volts rms and $\sigma^2 = 100$ gives the best performance. The obtained results are presented in Section 4.3.1.

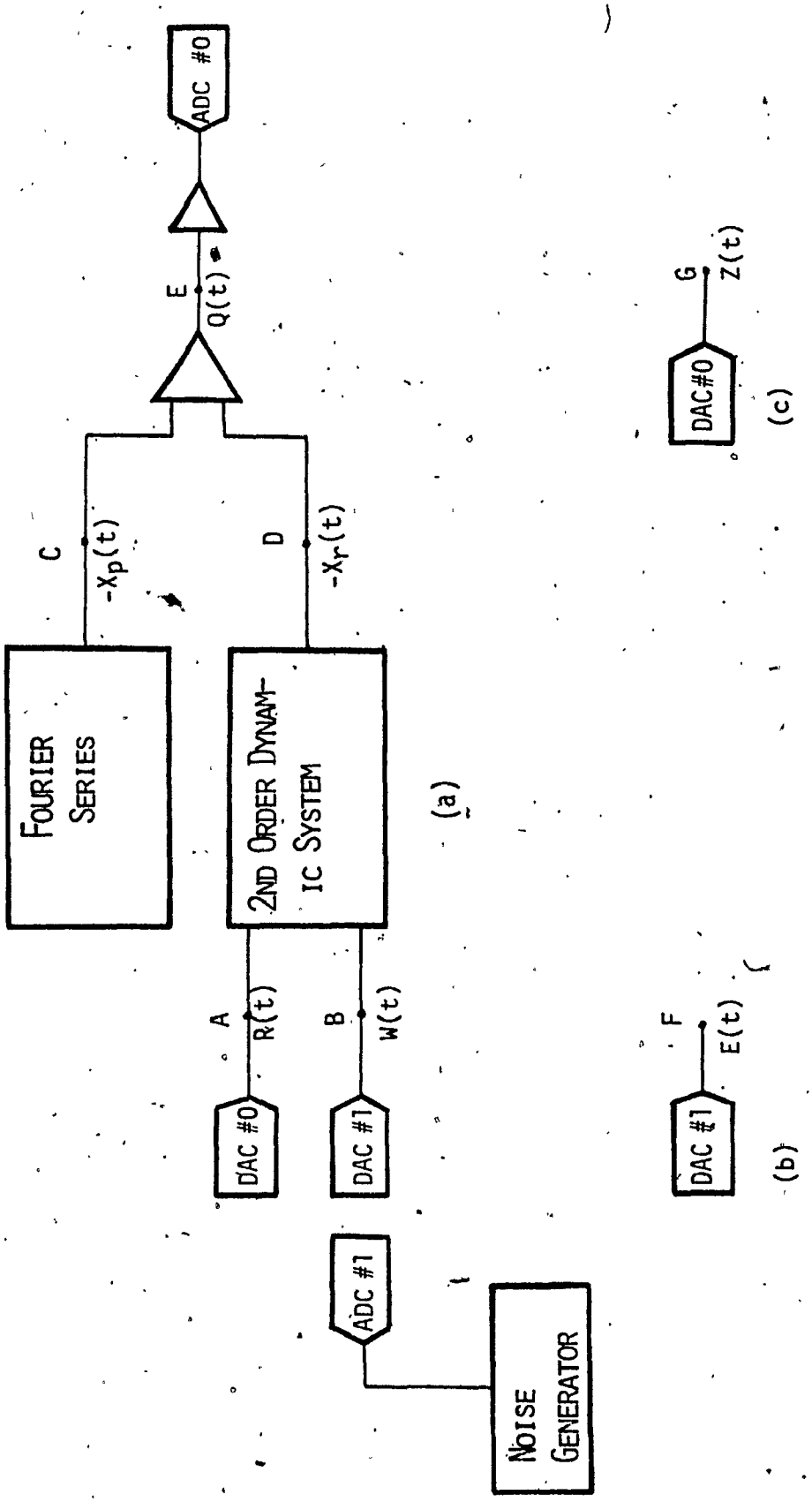

FIG. 4.11 - A SCHEMATIC DIAGRAM OF THE IMPLEMENTED MODEL SHOWING THE NODES AT WHICH THE VARIABLES ARE MEASURED.

4.3.1 Results of Simulation

The outputs obtained from the simulation of the load model for short-term forecasting are shown in Figures 4.12 through 4.18. In order to provide a complete picture, inputs and intermediate variables are also plotted. Figure 4.11 indicates the nodes at which the variables are measured.

The two inputs to the model are shown in Figures 4.12 and 4.13. Figure 4.12 shows the normalized temperature function R(t), as measured at point A in Figure 4.11, after it has been delayed by six units of time and supplied to the analog console through the D/A channel #0. Figure 4.13 shows a typical record of the Gaussian noise W(t), as it appears at point B in Figure 4.11, after its conversion through the D/A channel #1. Its variance is 100 and its rms magnitude is 0.4 volts. The two components of the simulated load are shown in Figure 4.15, as they appear with reversed signs at points C and D in Figure 4.11, respectively. The addition of $X_p(t)$ and $X_r(t)$ results in the normalized simulated load Q(t) at point E in Figure 4.11, as shown in Fig. 4.16. Figure 4.17 shows, for purposes of comparison, the load data used in this study. The load data Z(t) is supplied to the analog console through the D/A channel #0, as shown in Figure 4.11. Finally, the error E(t) is plotted in Figure 4.18, to show the discrepancies between the model and the actual system load.

4.3.2 Discussion of Results

In this section, we compare the hybrid simulated load with the actual load data, and to the digitally simulated load as obtained by Koutchouk.[28]

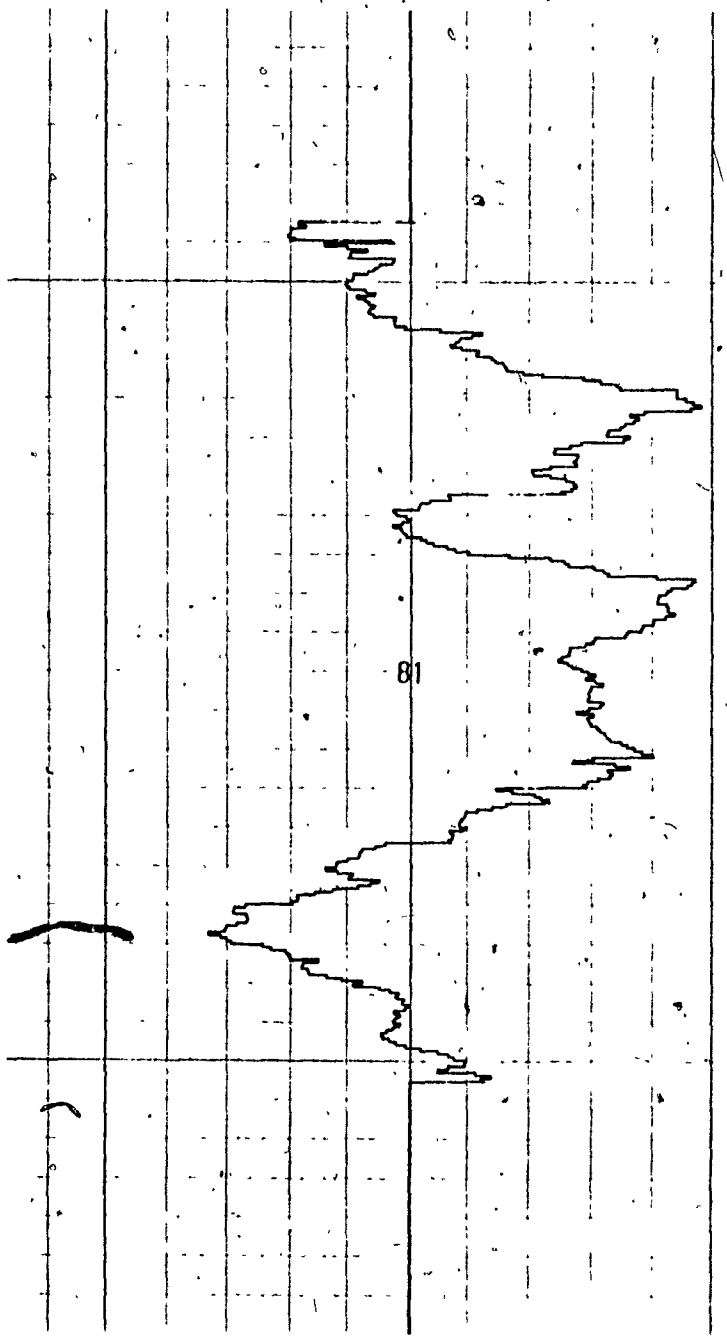

FIG. 4.12 - TEMPERATURE FUNCTION $\bar{R}(t)$

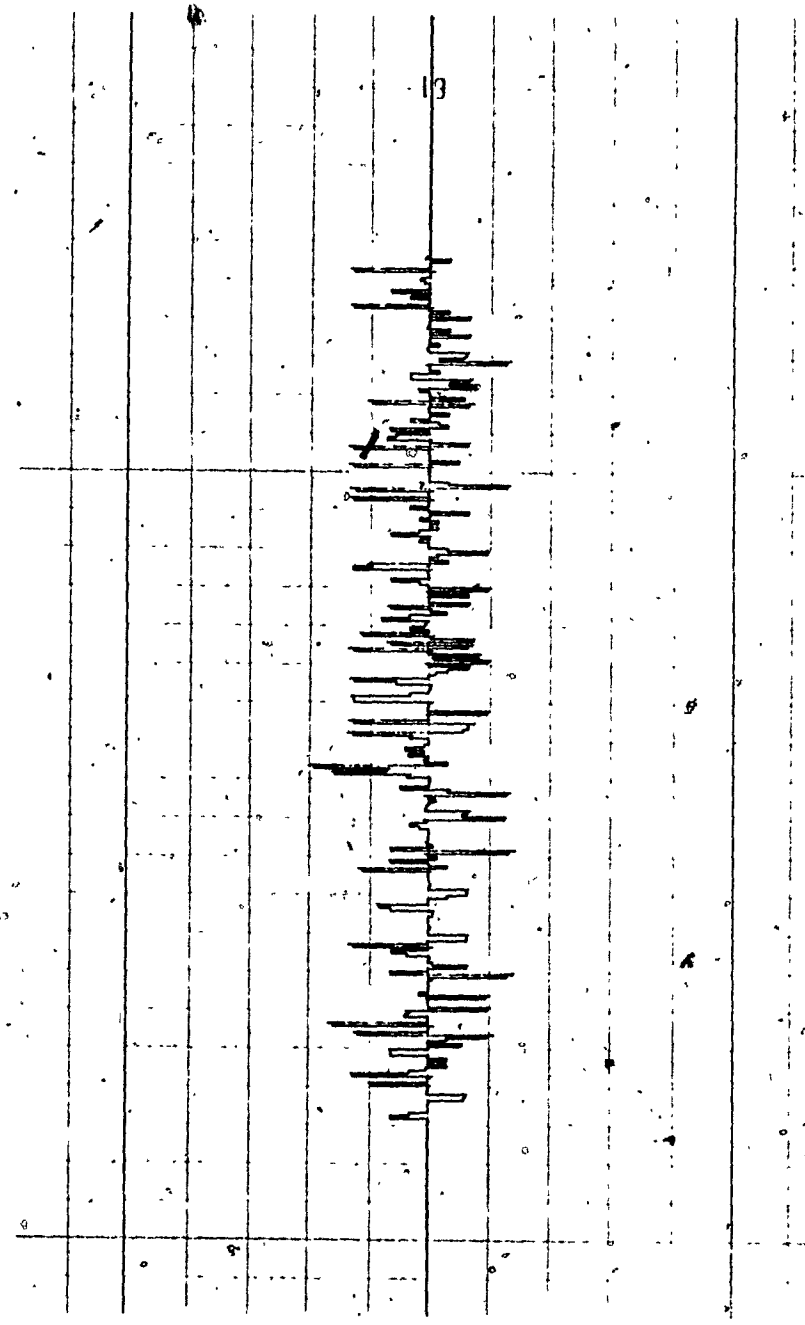

FIG. 4.13 - INPUT NOISE w(t)

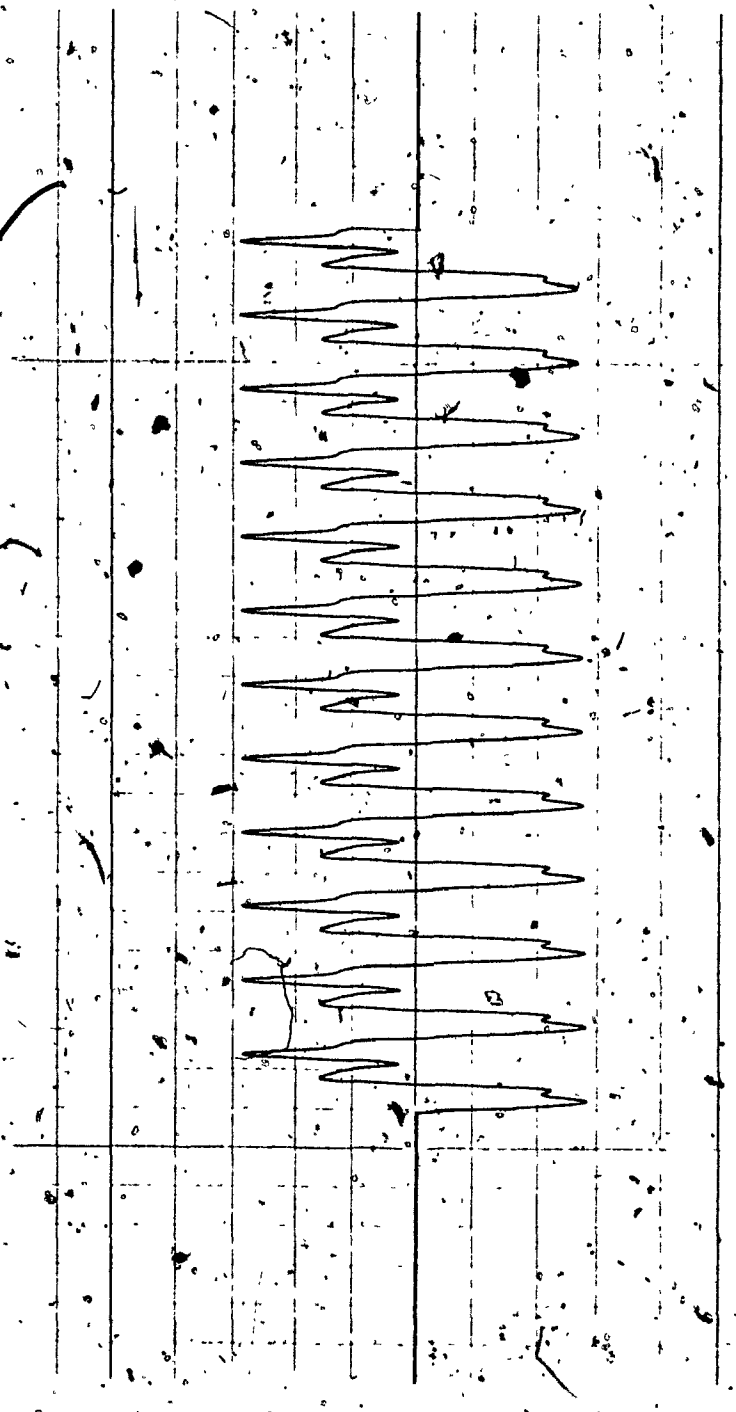

FIG. 4.14 - PERIODIC COMPONENT $x_p(t)$

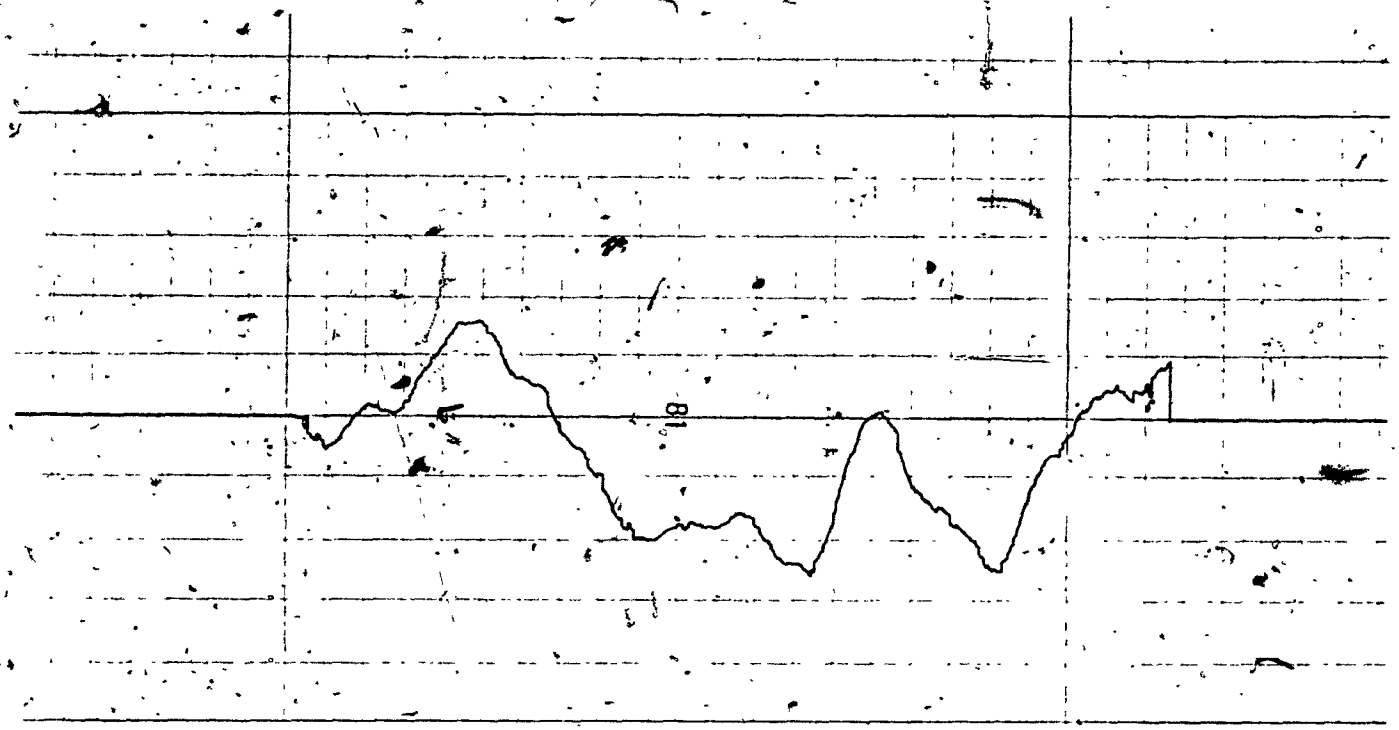

FIG. 4.15 - RESIDUAL COMPONENT $x_r(t)$

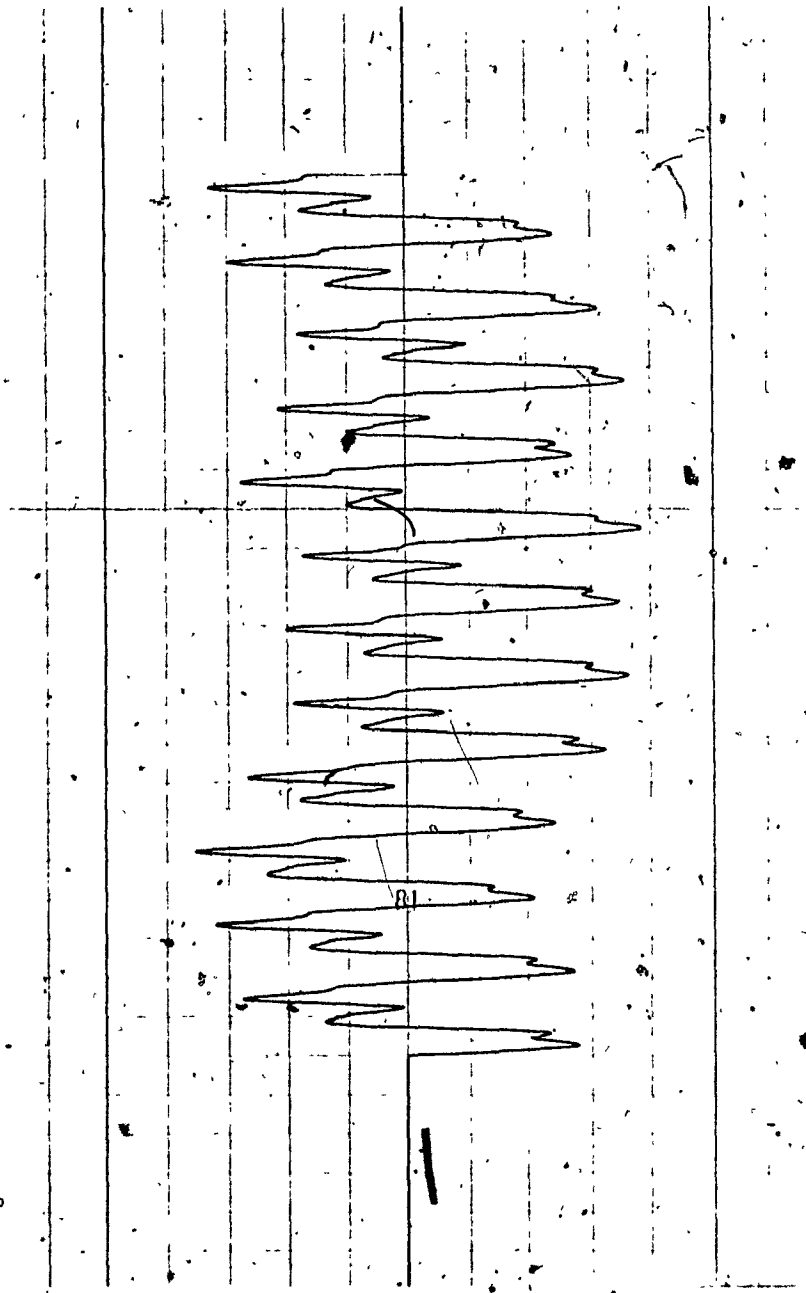

FIGURE 4.16 - SIMULATED LOAD Q(t)

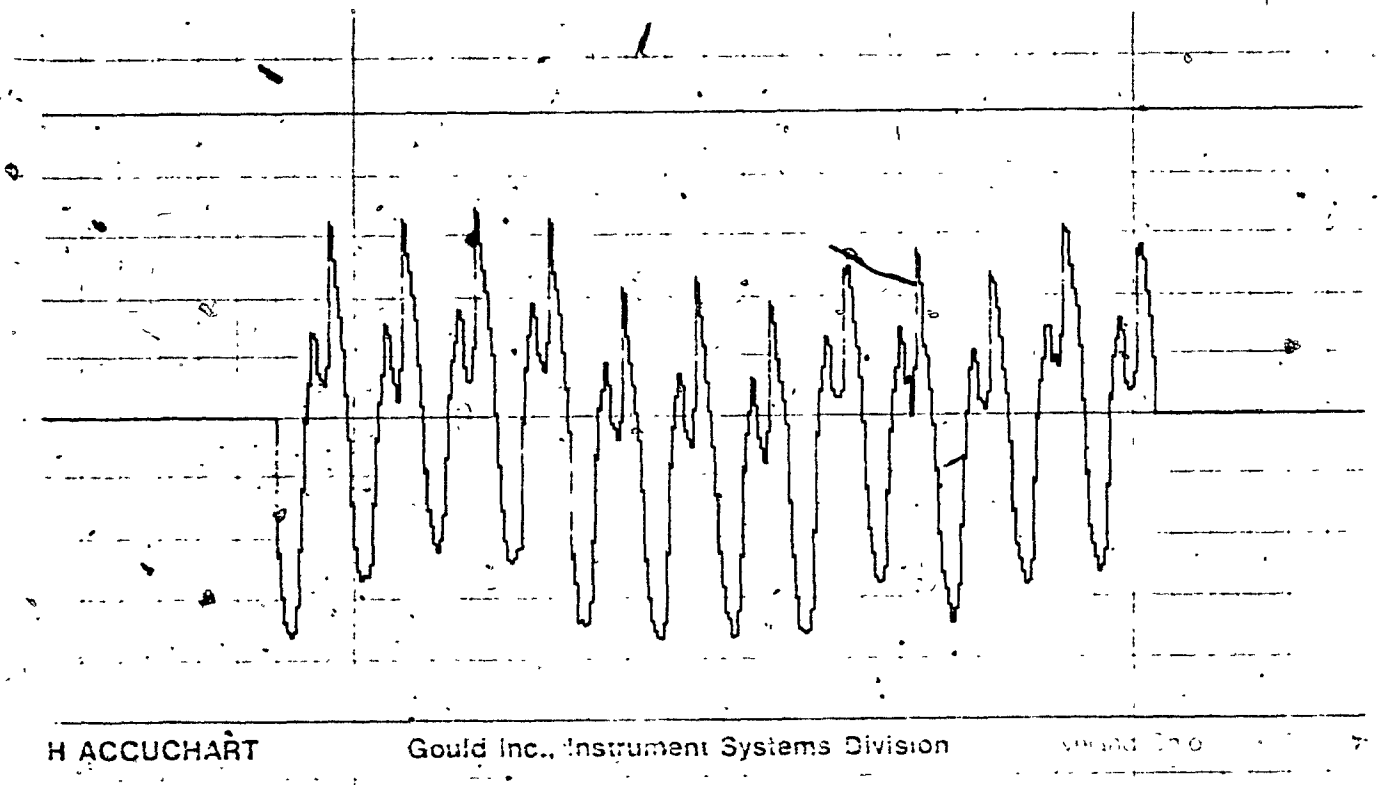

FIGURE 4.17 - LOAD DATA $z(t)$

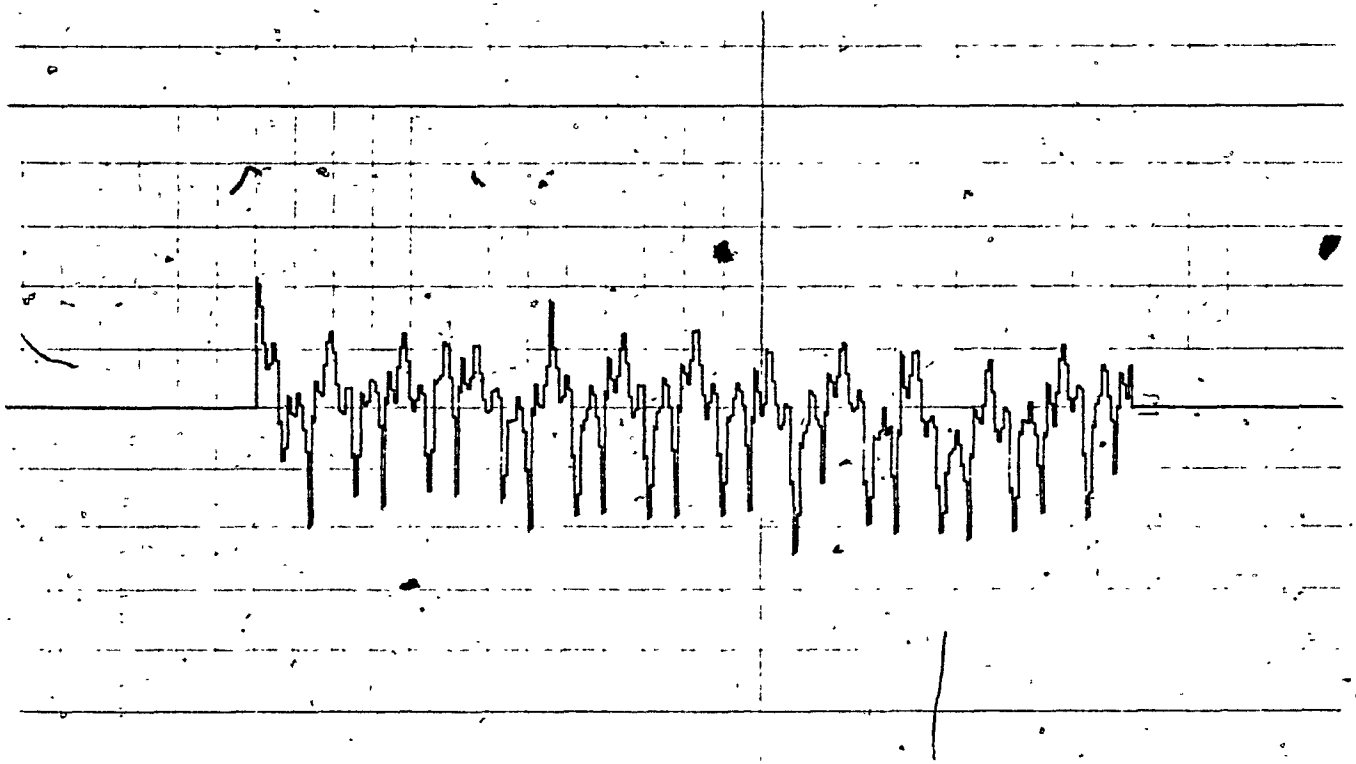

FIGURE 4.18 - ERROR E(t) = X(t) - Z(t)

Comparing first the hybrid simulated load with the actual load data, we observe three types of errors whose magnitude is significant. These errors are respectively: (i) peak errors, (ii) valley errors, and (iii) 20th hour errors.

(i) PEAK ERRORS

A good visualization of the peak errors is obtained from the error E(t) as shown in Figure 4.18. It is obvious that the largest errors occur at the load peaks of every day. During the morning and afternoon peaks, the observed errors have approximately the same magnitude, varying from 6% to 11% of the total load. These numbers show that peak errors do not greatly depend on the nature of the peak (morning or afternoon). On the contrary, their magnitude depends on how fast the load reaches its peak. Since these errors occur every peak period, it is obvious that peak errors do not depend on temperature changes and therefore on the accuracy of the residual component. Rather, it is thought that the inclusion of higher harmonics in the periodic component $Y_p(t)$ will yield more accurate results.

(ii) VALLEY ERRORS

Valley errors occur during the late and first hours of each day. In particular, from the 23rd hour of the ith day until the 3rd hour of the i + 1 day, it is noted that there is on the average a discrepancy about 6% of the total load. The source of these errors is identified by observing the actual load data (Figure 4.17) and the simulated load (Figure 4.16). As seen from Figure 4.16, the simulated load follows a ripple at the hours mentioned above, while the actual load data increases

smoothly at this time. Therefore it is evident that the valley errors are also caused by an inadequate number of harmonics in the periodic component, $Y_p(t)$.

(iii) 20th HOUR ERRORS

This error occurs exactly on the 20th hour of each day. Its magnitude vaires from 3% to about 6% of the total load. As seen from Figures 4.14 and 4.16, this error is introduced by the periodic component $Y_p(t)$ in an effort to produce a keen afternoon peak. Hence, a correction of these errors can be made by increasing the number of harmonics accordingly.

In summary, we see that all major errors are due to the inaccuracy of the periodic component $Y_p(t)$. This dictates the use of higher harmonics in the Fourier series (4.37). The accuracy of the residual component $Y_r(t)$ is considered, in general, to be satisfactory. Large discrepancies due to this component are noted in the 1st, 8th, and 12th days of the simulation. By increasing the order of the sub-system B (see Figure 3.1) from 2 to 3, the accuracy of $Y_r(t)$ can be increased considerably. The overall performance of the model is measured by the Average Absolute Error which was found to be 291 MW corresponding to 2.91% of the average total load.

A comparison of the results obtained from the hybrid simulation with the results obtained through the digitally simulated load, as obtained by Koutchouk,[29] shows the existence of the same discrepancies between the performances of the two models. The only difference is that the errors between the actual load and the hybrid model are larger than the errors between the digital model and the hybrid model. This is due

to the fact that simulation on the analog computer does not follow the high rates of load changes in the model, while simulation on the digital computer does. The conclusion that the inaccuracy of the periodic component $Y_p(t)$ is the main source of the errors is supported by the work of Koutchouk.[30] A discrete model with 8 harmonics and a 3rd order dynamic system gave a 3% peak error. Due to limited number of integrators on the EAI 680 analog computer, this model was not tested.

CHAPTER 5
CONCLUSIONS

The objective of this study was to simulate on a hybrid computer an electric power load over a 12 day period. The following concluding remarks summarize the advantages and disadvantages characterizing the load model and its hybrid simulation.

(1) Decomposition of the load into periodic and residual components provides a simple structure for the load model, which facilitates its implementation and furthermore provides a clear picture of the load behaviour during its simulation.

(2) The performance of the load model requires a hybrid computer, since inputs to the model are of discrete form, and only continuous time simulation of the model resembles the actual system load.

(3) The performance of the load model provides a simulated load whose discrepancies from the actual load are mainly at the load peaks and valleys. Peak errors vary from 6% to 11% while valley errors are about 6% of the total load. An overall measure of the performance is the average absolute error which is found to be 2.91% of the average total load. These errors are due to an insufficient number of harmonics describing the periodic component of the model. The residual component performs very well in comparison with the

performance of the periodic component.

Source error identification dictates two basic improvements which would make the model more accurate:

(1) To increase the number of harmonics in the Fourier series describing the periodic component, thus improving the model's accuracy at the load peaks and valleys, and

(2) To increase the order of the dynamic system describing the residual component, thus improving the model's response to temperature variations.

It is considered worthwhile to continue this work in areas such as,

(1) simulation of a more accurate model, by employing more integrators on the hybrid system

(2) sensitivity studies of the model to small parameter variations, and

(3) on-line use of the hybrid system for short-term electric load forecasting.

FOOTNOTES

[1]Galiana, F.D., "An Application of System Identification and State Prediction to Electric Load Modelling and Forecasting", Doctoral Thesis, M.I.T., 1971.

[2]Koutchouk, J.P. and Panuska, V., "Electrical Power System Load Modelling by a Two-Stage Stochastic Approximation Procedure", Internal Report, Sir George Williams University, 1974.

[3]Dryar, H.A., "Effect of Weather on the System Load", Transactions of the American I.E.E., 63, p. 1006, 1944.

[4]Davies, M., "The Relationship Between Weather and Electricity Demand", Proc. I.E.E., Vol. 106C, p. 27, 1958.

[5]Heinemann, G.T. et al, "The Relationship Between Summer Weather and Summer Loads - A Regression Analysis", IEEE Transactions on Power Apparatus and Systems, Vol. PAS-85, No. 11, p. 1144, 1966.

[6]Galiana, op. cit.

[7]Latham, J.H. et al, "Probability Approach to Electric Utility Load Forecasting", IEEE Transactions on Power Apparatus and Systems, Vol. PAS-87, No. 2, p. 496, 1968.

[8]Matthewman, P.D. and Nicholson, H., "Techniques for Load Prediction in the Electric Power Supply Industry", PROC. IEE, Vol. 115, No. 10, 1968.

[9]Farmer, E.D. and Potton, M.J., "Development of On-Line Load Prediction Techniques with Results from Trials in the Southwest Region of the CEGB", Proc. IEE, Vol. 115, 1968.

[10]Y. Inoue and J. Toyoda, "AM Application of Sequential Filter to Power Systems and Separation Algorithms of System Noise and Observation Noise", presented at the IEE (Japan) Spring Meeting, Tokyo, Japan, 1969.

[11]Schweppe, F.C. and Wildes, J., "Power System Static State Estimation, Part I: Exact Model", IEEE Transactions on Power Apparatus and Systems, Vol. PAS-89, p. 120, 1970.

[12]Toyoda, J. et al, "An Application of State Estimation to Short-Term Load Forecasting, Part I: Forecasting Modeling, Part II: Implementation", IEEE Transactions on Power Apparatus and Systems, Vol. PAS-89, No. 7, pp. 1678 - 1686, 1970.

[13]Larson, R.E. et al, "State Estimation in Power Systems, Part I: Theory and Feasibility", IEEE Transactions on Power Apparatus and Systems, Vol. PAS-89, p. 345, 1970.

[14]Christiaanse, W.R., "Short-Term Load Forecasting Using General Exponential Smoothing", IEEE Transactions on Power Apparatus and Systems, Vol. PAS-90, No. 2, p. 900, 1971.

[15]Galiana, op. cit.

[16]Koutchouk, op. cit.

[17]Davey, J., et al, "Practical Application of Weather Sensitive Load Forecasting to System Planning", IEEE Transactions on Power Apparatus and Systems, Vol. PAS-92, p. 971, 1973.

[18]Corpening, S.L. et al, "Experience with Weather Sensitive Load Models for Short-Term Forecasting", IEEE Transactions on Power Apparatus and Systems, Vol. PAS-92, p. 1966, 1973.

[19]Dryar, op. cit.

[20]Davies, op. cit.

[21]Galiana, op. cit.

[22]Koutchouck, op. cit.

[23]Dryar, op. cit.

[24]Galiana, op. cit.

[25]Galiana, op. cit.

[26]Koutchouk and Panuska, op. cit.

[27]Koutchouk and Panuska, op. cit.

[28]Koutchouk, op. cit.

[29]Koutchouk, op. cit.

[30]Koutchouk, op. cit.

S E L E C T E D B I B L I O G R A P H Y

BEKEY, G.A. and KARPLUS, W.J. Hybrid Computation, John Wiley, New York, 1968.

CHRISTIAANSE, W.R. "Short-Term Load Forecasting Using General Exponential Smoothing", IEEE Transactions on Power Apparatus and Systems, Vol. PAS-89, 1970.

CORPENING, S.L. et al, "Experience with Weather Sensitive Load Models for Short-Term Forecasting", IEEE Transactions on Power Apparatus and Systems, Vol. PAS-92, 1973.

DAVEY, J. et al. "Practical Application of Weather Sensitive Load Forecasting to System Planning", IEEE Transactions on Power Apparatus and Systems, Vol. PAS-92, 1973.

DAVIES, M. "The Relationship Between Weather and Electricity Demand", Proc. IEE Vol. 106C, p. 27, 1958.

DRYAR, H.A. "Effect of Weather on the System Load", Transactions of the American IEE 63, p. 1006, 1944.

EAI 640 Scientific Computing System, Reference Handbook, June 1969.

EAI 680 Scientific Computing System, Reference Handbook, Oct. 1966.

EAI 690 Hybrid Computing System, Reference Handbook, March, 1969.

FARMER, E.D. and POTTON, M.J. "Development of On-Line Load Prediction Techniques with Results from Trials in the Southwest Region of the CEGB", Proc. IEE, Vol. 115, 1968.

GALIANA, F.D. "An Application of System Identification and State Prediction to Electric Load Modelling and Forecasting", Doctoral Thesis, M.I.T., 1971.

GIRGENTI, J.C. "Identification de la Charge a Court Terme d'un Reseau Electrique", Internal Report, Sir George Williams University, 1973.

HARGREVES, D.R. and PANUSKA, V. "Modelling of Electric Power System Load by Stochasting Approximation", Canadian Conference on Automatic Control, Fredericton, N.B. 1973.

HEINEMANN, G.T. et al. "The Relationship Between Summer Weather and Summer Loads - A Regression Analysis", IEEE Transactions on Power Apparatus and Systems, Vol. PAS-85, No. 11, p. 1144, 1966.

INOUE, Y. and TOYODA, J. "An Application of Sequential Filter to Power Systems and Separation Algorithms of System Noise and Observation Noise", presented at the IEE (Japan) Spring Meeting, Tokyo, Japan, 1969.

KOUTCHOUK, J.P. and PANUSKA, V. "Electrical Power System Load Modelling by a Two-Stage Stochastic Approximation Procedure", Internal Report, Sir George Williams University, 1974.

LARSON, R.E. et al. "State Estimation in Power Systems, Part I: Theory and Feasibility", IEEE Transactions on Power Apparatus and Systems, Vol. PAS-89, 1970.

LATHAM, J.H. et al. "Probability Approach to Electric Utility Load Forecasting", IEEE Transactions on Power Apparatus and Systems, Vol. PAS-87, No. 2, p. 496, 1968.

LEVINE, L. Methods for Solving Engineering Problems Using Analog Computers, John Wiley, New York, 1966.

MATTEWMAN, P.D. and Nicholson, H. "Techniques for Load Prediction in the Electric Power Supply Industry", PROC. IEE, Vol. 115, No. 10, 1968.

SCHWEPPE, F.C. and WILDES, J. "Power System Static State Estimation, Part I: Exact Model", IEEE Transactions on Power Apparatus and Systems, Vol. PAS-89, 1970.

SOLINAS, J. "Needs, Applications and Techniques of Load Forecasting Applied to Operating and Controlling a Power Utility", M. Eng., Sir George Williams University, Montreal, 1973.

TOYODA, J. et al. "An Application of State Estimation to Short-Term Load Forecasting, Part I: Forecasting Modelling, Part II: Implementation", IEEE Transactions on Power Apparatus and Systems, Vol. PAS-89, No. 7, 1970.

APPENDIX A

SAMPLE COMPUTER PROGRAMS FOR THE HYBRID SIMULATION

PROGRAM POTSET

```
      DIMENSION P(33),V(33)
      DATA P(1)/4HP000/,P(2)/4HP001/,P(3)/4HP002/,P(4)/4HP003/,
     1P(5)/4HP004/,P(6)/4HP005/,P(7)/4HP006/,P(8)/4HP007/,
     1P(9)/4HP008/,P(10)/4HP010/,P(11)/4HP015/,P(12)/4HP016/,
     1P(13)/4HP031/,P(14)/4HP032/,P(15)/4HP033/,P(16)/4HP035/,
     1P(17)/4HP036/,P(18)/4HP037/,P(19)/4HP038/,P(20)/4HP042/,
     1P(21)/4HP045/,P(22)/4HP062/,P(23)/4HP064/,P(24)/4HP065/,
     1P(25)/4HP066/,P(26)/4HP067/,P(27)/4HP068/,P(28)/4HP070/,
     1P(29)/4HP091/,P(30)/4HP094/,P(31)/4HP095/,P(32)/4HP096/,
     1P(33)/4HP034/
      DATA V(1)/.0105/,V(2)/.1112/,V(3)/.0450/,V(4)/.9999/,
     1V(5)/.1275/,V(6)/.9999/,V(7)/.0924/,V(8)/.3000/,V(9)/.0337/,
     1V(10)/.0091/,V(11)/.7850/,V(12)/.7850/,V(13)/.0210/,
     1V(14)/.5233/,V(15)/.5233/,V(16)/.0052/,V(17)/.6542/,
     1V(18)/.0019/,V(19)/.0118/,V(20)/.6542/,V(21)/.0027/,
     1V(22)/.2617/,V(23)/.2617/,V(24)/.0413/,V(25)/.3925/,
     1V(26)/.0105/,V(27)/.0192/,V(28)/.3925/,V(29)/.1308/,
     1V(30)/.0288/,V(31)/.1308/,V(32)/.0210/,V(33)/.1000/
      CALL QSHYIN(IER,680)
      DO 50 L=1,3
      DO 30 K=1,33
   30 CALL QWPR(P(K),V(K),IER)
   50 CONTINUE
      END
```

```
*****************************************************************
                        S E C T I O N   2.

      THE FOLLOWING 3 STATEMENTS ARE USED FOR INITILIZATION

      CALL QWJDAR(0.,0,IER)
      CALL QWJDAR(0.,1,IER)
      I=1

      THE FOLLOWING 27 STATEMENTS EXECUTE THE SIMULATION
                        OF THE MODEL

      CALL QWCLL(0,.TRUE.,IER)
      CALL QRBADR(W,1,1,IER)
      CALL QWJDAR(W,1,IER)
      CALL QRBADR(A,0,1,IER)
      X(I)=A*9480.+7366.
    3 I=I+1
      CALL QRSLL(0,SENS,IER)
    7 CALL QRSLL(0,SENS,IER)
      IF(.NOT.SENS)GO TO 7
      CALL QRBADR(W,1,1,IER)
      CALL QWJDAR(W,1,IER)
      CALL QRBADR(A,0,1,IER)
      X(I)=A*9480.+7366.
      IF(I.EQ.6) GO TO 8
      GO TO 3
    8 I=I+1
      CALL QRSLL(0,SENS,IER)
    4 CALL QRSLL(0,SENS,IER)
      IF(.NOT.SENS)GO TO 4
      U1=U(I-6)*.0003449
      CALL QRBADR(W,1,1,IER)
      CALL QWJDAR(W,1,IER)
      CALL QWJDAR(U1,0,IER)
      CALL QRBADR(A,0,1,IER)
      X(I)=A*9480.+7366.
      IF(I.EQ.288)GO TO 5
      GO TO 6

      THE FOLLOWING 4 STATEMENTS RE-INITIALIZE THE PROCESS

    5 CALL QWJDAR(0.,0,IER)
      CALL QWJDAR(0.,1,IER)
      CALL QWCLL(0,.FALSE.,IER)
      I=0
      PAUSE 3
*****************************************************************
```

```
**********************************************************************
                    S E C T I O N  3.

      THE FOLLOWING 10 STATEMENTS CALCULATE THE ERROR AND FEED IT
      TO THE ANALOG TOGETHER WITH THE LOAD DATA FOR PLOTTING

      CALL QWCLL(0,.TRUE.,IER)
   11 I=I+1
      CALL QRSLL(0,SENS,IER)
    9 CALL QRSLL(0,SENS,IER)
      IF(.NOT.SENS)GO TO 9
      E(I)=X(I)-Z(I)
      A=E(I)*.0001
      CALL QWJDAR(A,1,IER)
      ZI=(Z(I)-7300.)/9480.
      CALL QWJDAR(ZI,0,IER)
      IF(I.LT.288)GO TO 11

      THE FOLLOWING 3 STATEMENTS RE-INITIALIZE THE PROCESS

      CALL QWJDAR(0.,0,IER)
      CALL QWJDAR(0.,1,IER)
      CALL QWCLL(0,.FALSE.,IER)
      PAUSE 4
**********************************************************************
```

```
C*************************************************************
C                    S E C T I O N  4.
C
C     THE FOLLOWING 7 STATEMENTS ARE USED TO INITIALIZE THE INDECES.
C
      L=1
      K=24
      NFD=-1
      NSD=0
   31 NHOUR=0
      NFD=NFD+2
      NSD=NSD+2
C
C        THE FOLLOWING 13 STATEMENTS OUTPUT THE TEMPERATURE,
C        SIMULATED AND LOAD DATA AND THE ERROR,
C        FOR EVERY DAY AND EVERY HOUR IN THE SIMULATION.
C
      TYPE 24, NFD,NSD
   24 FORMAT(//,20X,8HDAY  NO.,I2,21X,8HDAY  NO.,I2,//,1HX,
     159HHOUR  U(I)  Z(I)  X(I)  E(I)   HOUR  U(I)  Z(I)  X(I)  E(I),)
      DO 30 I=L,K
      NHOUR=NHOUR+1
      II=I+24
      TYPE 13, NHOUR,U(I),Z(I),X(I),E(I),NHOUR,U(II),Z(II),X(II),E(II)
   13 FORMAT(12X,I2,1X,F6.1,1X,3F6.0,3X,I2,1X,F6.1,1X,3F6.0)
   30 CONTINUE
      IF(K.EQ.264)GO TO 32
      L=L+48
      K=K+48
      GO TO 31
C
C        THE FOLLOWING 6 STATEMENTS CALCULATE AND OUTPUT THE
C                    ABSOLUTE AVERAGE ERROR
C
   32 B=0.
      DO 40 I=1,288
   40 B=B+ABS(E(I))
      A=B/288.
      TYPE 23, A
   23 FORMAT(////,17X,30HAVERAGE   ABSOLUTE   ERROR =  ,F6.0,////)
      GO TO 60
      END
C*************************************************************
```

APPENDIX B

DIGITAL OUTPUT OBTAINED FROM THE HYBRID SIMULATION

DAY NO. 1

HOUR	U(T)	Z(T)	X(T)	E(T)
1	-8.2	6329.	7330.	1001.
2	-9.5	5995.	6811.	816.
3	-7.5	5809.	6352.	543.
4	-2.8	5738.	6065.	327.
5	-4.1	5699.	6079.	380.
6	-6.2	5742.	6287.	545.
7	-6.4	5926.	6329.	403.
8	-4.8	6345.	6235.	-109.
9	-4.1	6798.	6403.	-394.
10	-2.7	7330.	7023.	-306.
11	-.6	7617.	7690.	73.
12	.6	8005.	7957.	-47.
13	1.7	7966.	7893.	-72.
14	2.4	7703.	7810.	107.
15	3.1	7656.	7661.	5.
16	3.2	7606.	7430.	-175.
17	2.6	7752.	7398.	-353.
18	1.9	8830.	7864.	-965.
19	1.2	8576.	8463.	-112.
20	1.9	8384.	8592.	208.
21	1.7	8143.	8270.	127.
22	1.2	7982.	7975.	93.
23	1.8	7540.	7898.	358.
24	.6	7198.	7750.	552.

DAY NO. 2

HOUR	U(T)	Z(T)	X(T)	E(T)
1	.2	6717.	7342.	625.
2	.9	6371.	6829.	458.
3	.8	6187.	6373.	186.
4	1.6	6118.	6089.	-28.
5	1.4	6159.	6106.	-52.
6	2.4	6144.	6301.	157.
7	3.5	6235.	6403.	168.
8	6.3	6699.	6329.	-369.
9	5.2	7135.	6476.	-708.
10	7.7	7477.	7097.	-379.
11	9.7	7687.	7709.	102.
12	11.9	8071.	8086.	15.
13	12.1	7993.	8041.	48.
14	12.8	7741.	7967.	226.
15	12.6	7620.	7827.	207.
16	10.7	7486.	7605.	119.
17	14.2	7733.	7588.	-144.
18	14.4	8854.	8062.	-791.
19	14.8	8620.	8659.	39.
20	16.4	8492.	8798.	298.
21	17.2	8314.	8457.	143.
22	20.8	8113.	8148.	35.
23	21.4	7767.	8092.	325.
24	22.1	7451.	7957.	506.

DAY NO. 3

HOUR	U(T)	Z(T)	X(T)	E(T)
1	23.7	6946.	7565.	619.
2	21.5	6662.	7052.	390.
3	21.4	6538.	6611.	73.
4	20.1	6396.	6375.	-20.
5	18.8	6330.	6403.	73.
6	18.8	6427.	6616.	189.
7	19.0	6625.	6736.	111.
8	20.7	7035.	6673.	-361.
9	20.4	7508.	6833.	-674.
10	19.0	7792.	7441.	-350.
11	14.1	7936.	8133.	197.
12	13.2	8196.	8420.	224.
13	13.4	8113.	8368.	255.
14	11.1	7747.	8282.	535.
15	8.8	7631.	8148.	517.
16	5.8	7646.	7894.	248.
17	4.4	7893.	7815.	-78.
18	3.5	8940.	8247.	-692.
19	6.0	8697.	8824.	127.
20	6.2	8502.	8916.	414.
21	8.2	8344.	8551.	207.
22	9.8	8042.	8191.	149.
23	8.4	7833.	8083.	250.
24	8.2	7393.	7901.	508.

DAY NO. 4

HOUR	U(T)	Z(T)	X(T)	E(T)
1	6.0	6976.	7502.	526.
2	5.6	6657.	6938.	281.
3	5.4	6418.	6486.	68.
4	5.2	6263.	6227.	-35.
5	3.0	6244.	6222.	-21.
6	2.7	6270.	6417.	138.
7	-4.1	6351.	6506.	155.
8	-4.7	6361.	6440.	79.
9	-4.8	7310.	6588.	-729.
10	-4.4	7719.	7180.	-538.
11	-6.5	7980.	7864.	-115.
12	-7.5	8250.	8154.	-95.
13	-7.5	8133.	8046.	-86.
14	-5.9	7844.	7933.	89.
15	-6.2	7773.	7777.	-5.
16	-6.4	7704.	7514.	-189.
17	-7.8	7933.	7440.	-492.
18	-9.7	8852.	7864.	-987.
19	-11.2	8469.	8433.	-36.
20	-15.9	8357.	8551.	194.
21	-14.9	8158.	8180.	22.
22	-14.3	7854.	7858.	4.
23	-11.7	7578.	7757.	179.
24	-10.0	7251.	7597.	346.

DAY NO. 5

HOUR	U(T)	Z(T)	X(T)	E(T)
1	-19.8	6311.	7160.	849.
2	-20.2	6088.	6597.	509.
3	-21.5	5901.	6139.	338.
4	-23.0	5918.	5870.	52.
5	-23.3	5780.	5880.	100.
6	-22.5	5794.	6060.	266.
7	-25.3	5950.	6093.	143.
8	-23.5	6400.	6032.	-367.
9	-18.6	7023.	6148.	-874.
10	-20.9	7413.	6713.	-699.
11	-27.8	7570.	7389.	-180.
12	-26.7	7773.	7661.	-111.
13	-25.8	7602.	7588.	-13.
14	-24.9	7313.	7486.	173.
15	-24.1	7270.	7368.	98.
16	-23.0	7180.	7111.	-68.
17	-22.4	7328.	7023.	-304.
18	-22.2	8323.	7468.	-854.
19	-21.7	7975.	8051.	76.
20	-21.3	7767.	8180.	413.
21	-20.6	7595.	7927.	232.
22	-20.5	7388.	7519.	131.
23	-20.2	7174.	7442.	268.
24	-20.9	6798.	7301.	503.

DAY NO. 6

HOUR	U(T)	Z(T)	X(T)	E(T)
1	-19.0	6265.	6884.	619.
2	-20.4	5975.	6346.	371.
3	-21.7	5813.	5917.	104.
4	-22.0	5735.	5676.	-59.
5	-20.2	5696.	5694.	0.
6	-20.5	5674.	5875.	201.
7	-20.5	5794.	5973.	179.
8	-20.6	6304.	5912.	-391.
9	-20.8	6954.	6056.	-897.
10	-22.1	7274.	6643.	-630.
11	-21.1	7514.	7345.	-168.
12	-20.1	7688.	7658.	-29.
13	-21.1	7594.	7605.	11.
14	-20.2	7256.	7503.	247.
15	-19.6	7185.	7356.	171.
16	-18.5	7117.	7116.	-1.
17	-18.0	7411.	7069.	-342.
18	-16.9	8401.	7523.	-877.
19	-17.4	8133.	8106.	-26.
20	-18.1	7994.	8235.	341.
21	-18.3	7619.	7900.	281.
22	-18.4	7396.	7598.	192.
23	-20.1	7119.	7514.	395.
24	-20.9	6762.	7389.	627.

DAY NO. 7

HOUR	U(T)	Z(T)	X(T)	E(T)
1	-21.1	6318.	6967.	649.
2	-24.7	6059.	6417.	358.
3	-25.1	5870.	5975.	105.
4	-26.6	5823.	5736.	-86.
5	-26.8	5690.	5736.	46.
6	-28.1	5703.	5894.	191.
7	-28.1	5882.	5986.	104.
8	-29.5	6282.	5917.	-364.
9	-30.6	6926.	6056.	-869.
10	-29.9	7218.	6606.	-611.
11	-29.8	7390.	7291.	-98.
12	-29.6	7645.	7588.	-56.
13	-29.6	7442.	7518.	76.
14	-28.6	7187.	7390.	203.
15	-29.8	7102.	7241.	139.
16	-29.7	6986.	7010.	24.
17	-30.2	7244.	6957.	-286.
18	-32.1	8211.	7382.	-828.
19	-32.6	8073.	7967.	-105.
20	-33.0	7795.	8095.	300.
21	-28.4	7616.	7747.	131.
22	-22.5	7478.	7416.	-61.
23	-22.1	7296.	7338.	42.
24	-20.9	6719.	7185.	466.

DAY NO. 8

HOUR	U(T)	Z(T)	X(T)	E(T)
1	-18.1	6287.	6745.	458.
2	-17.6	5975.	6181.	206.
3	-16.1	5750.	5769.	19.
4	-11.5	5734.	5565.	-169.
5	-6.8	5713.	5579.	-133.
6	-5.0	5741.	5766.	25.
7	-4.0	5888.	5902.	14.
8	-2.2	6470.	5883.	-586.
9	-1.4	7207.	6060.	-1146.
10	-.6	7551.	6678.	-872.
11	.7	7731.	7420.	-310.
12	1.0	7961.	7772.	-188.
13	1.2	7889.	7753.	-135.
14	2.1	7560.	7677.	117.
15	.9	7506.	7588.	82.
16	.1	7501.	7407.	-93.
17	.6	7553.	7405.	-147.
18	1.6	8460.	7856.	-603.
19	2.0	8524.	8476.	-47.
20	-.4	8358.	8629.	271.
21	-.7	8081.	8289.	208.
22	-1.9	7883.	7971.	88.
23	-4.6	7652.	7907.	255.
24	-4.1	7311.	7789.	478.

DAY NO. 9

HOUR	U(T)	Z(T)	X(T)	E(T)
1	-17.2	6814.	7368.	554.
2	-18.5	6499.	6782.	283.
3	-19.1	6304.	6343.	39.
4	-18.6	6125.	6106.	-18.
5	-17.8	6008.	6033.	-4.
6	-16.0	6099.	6241.	142.
7	-14.0	6200.	6242.	42.
8	-13.9	6768.	6181.	-587.
9	-16.1	7238.	6292.	-945.
10	-19.1	7548.	6824.	-723.
11	-18.7	7726.	7477.	-248.
12	-19.1	8031.	7782.	-248.
13	-19.2	7903.	7716.	-186.
14	-16.3	7601.	7592.	-8.
15	-16.6	7658.	7444.	-213.
16	-18.4	7357.	7201.	-155.
17	-19.5	7709.	7157.	-551.
18	-24.5	8598.	7578.	-1019.
19	-25.3	8387.	8152.	-234.
20	-22.4	7894.	8314.	420.
21	-22.7	7808.	7972.	164.
22	-24.1	7558.	7639.	81.
23	-24.6	7289.	7551.	262.
24	-25.7	6934.	7383.	449.

DAY NO.10

HOUR	U(T)	Z(T)	X(T)	E(T)
1	-26.3	6471.	6935.	464.
2	-25.2	6163.	6377.	214.
3	-26.9	6033.	5935.	-97.
4	-32.5	5917.	5690.	-226.
5	-33.8	5791.	5676.	-114.
6	-32.8	5891.	5819.	-71.
7	-31.9	6067.	5912.	-154.
8	-30.8	6508.	5880.	-627.
9	-30.8	7011.	6005.	-1005.
10	-30.8	7378.	6523.	-854.
11	-24.2	7707.	7180.	-526.
12	-23.6	7861.	7494.	-366.
13	-21.7	7758.	7440.	-317.
14	-19.8	7486.	7301.	-185.
15	-15.1	7461.	7162.	-298.
16	-12.8	7404.	6956.	-447.
17	-11.0	7536.	6954.	-581.
18	-10.9	8431.	7383.	-1047.
19	-10.7	8387.	7992.	-394.
20	-9.9	8187.	8166.	-20.
21	-9.5	7952.	7862.	-89.
22	-7.7	7703.	7568.	-134.
23	-8.1	7522.	7544.	22.
24	-6.0	7148.	7449.	301.

DAY NO.11

HOUR	U(T)	Z(T)	X(T)	E(T)
1	-4.5	6642.	7028.	386.
2	-5.3	6371.	6486.	115.
3	-5.8	6256.	6069.	-186.
4	-7.1	6160.	5883.	-276.
5	-8.4	6072.	5898.	-173.
6	-3.3	6092.	6079.	-12.
7	.6	6239.	6194.	-44.
8	1.9	6839.	6181.	-658.
9	1.9	7330.	6329.	-1000.
10	1.7	7617.	6882.	-734.
11	4.2	7784.	7565.	-218.
12	4.7	8030.	7936.	-93.
13	4.5	8035.	7914.	-120.
14	4.0	7764.	7808.	44.
15	4.7	7815.	7692.	-122.
16	5.0	7727.	7504.	-222.
17	5.9	7959.	7493.	-465.
18	4.0	8789.	7923.	-865.
19	5.1	8758.	8527.	-230.
20	6.8	8517.	8694.	177.
21	7.2	8336.	8363.	27.
22	6.8	8196.	8041.	-154.
23	6.2	7876.	7985.	109.
24	6.3	7474.	7861.	387.

DAY NO.12

HOUR	U(T)	Z(T)	X(T)	E(T)
1	4.7	6917.	7440.	523.
2	3.9	6516.	6864.	348.
3	3.4	6366.	6433.	67.
4	2.0	6263.	6231.	-31.
5	1.8	6163.	6238.	75.
6	6.7	6208.	6392.	184.
7	6.6	6326.	6476.	150.
8	4.9	6810.	6454.	-355.
9	7.0	7471.	6579.	-891.
10	9.9	7797.	7106.	-690.
11	2.2	7935.	7782.	-152.
12	13.6	8101.	8134.	33.
13	14.5	7900.	8000.	99.
14	14.1	7605.	7949.	344.
15	14.0	7545.	7838.	293.
16	12.2	7577.	7655.	78.
17	13.1	7679.	7568.	-110.
18	13.4	8590.	8059.	-530.
19	15.6	8671.	8659.	-11.
20	14.3	8558.	8833.	275.
21	14.7	8319.	8504.	185.
22	14.5	8106.	8180.	74.
23	17.9	7790.	8120.	330.
24	20.0	7522.	8019.	497.

AVERAGE ABSOLUTE ERROR = 291.